Epstein, A. J., Rommelmann, H., Abkowitz, M. & Gibson, H. W. (1981). *Mol. Cryst. Liq. Cryst.* **77**, 81–96.

Gupta, R. R. (1986). Landolt-Börnstein, *New Series II*/16, edited by K.-H. Hellwege & A. M. Hellwege, pp. 176–177, 436–437. Berlin: Springer.

Keller, H. J., Nöthe, D., Pritzkow, H., Wehe, D., Werner, M., Koch, P. & Schweitzer, D. (1980). *Mol. Cryst. Liq. Cryst.* **62**, 181–200.

Kivelson, S. (1982). *Phys. Rev. B*, **25**, 3798–3821.

Raible, Ch., Gmeiner, J., Winter, H., Dormann, E., Stenger-Smith, J. D. & Enkelmann, V. (1993). *Synth. Met.* **59**, 71–80.

Riess, W., Brütting, W. & Schwoerer, M. (1993). *Synth. Met.* **55–57**, 2664–2669.

Sheldrick, G. M. (1995). *SHELX92. An Integrated System for Solving, Refining and Displaying Crystal Structures from Diffraction Data. J. Appl. Cryst.* In preparation.

Acta Cryst. (1994). **B50**, 746–762

The Influence of the Nitro Group on the Solid-State Structure of 4-Nitropyrazoles: the Cases of Pyrazole, 3,5-Dimethylpyrazole, 3,5-Di-*tert*-butylpyrazole and 3,5-Diphenylpyrazole. I. Static Aspects (Crystallography and Thermodynamics)

By Antonio L. Llamas-Saiz, Concepción Foces-Foces and Félix H. Cano

Departamento de Cristalografía, Instituto de Química-Física 'Rocasolano', CSIC, Serrano 119, *E*-28006 *Madrid, Spain*

Pilar Jimémez and José Laynez

Instituto de Química-Física 'Rocasolano', CSIC, Serrano 199, *E*-28006 *Madrid, Spain*

Wim Meutermans and José Elguero

Instituto de Química Médica, CSIC, Juan de la Cierva 3, *E*-28006 *Madrid, Spain*

and Hans-Heinrich Limbach and Francisco Aguilar-Parrilla

Institut für Organische Chemie, Fachbereich Chemie, Freie Universität Berlin, Takustrasse 3, *D*-14195 *Berlin, Germany*

(*Received* 31 *January* 1994; *accepted* 19 *April* 1994)

Abstract

We have determined the enthalpies of sublimation of 3,5-di-*tert*-butylpyrazole (3), 3,5-diphenylpyrazole (4), 4-nitropyrazole (5), 3,5-dimethyl-4-nitropyrazole (6), 3,5-di-*tert*-butyl-4-nitropyrazole (7) and 3,5-diphenyl-4-nitropyrazole (8); those of pyrazole (1) and 3,5-dimethylpyrazole (2) were already known. The effect of the C-substituents (Me, Bu^t, Ph and NO_2) on the enthalpies of sublimation of pyrazoles and benzenes are additive and linearly related. Moreover, we report the structure of three of these 4-nitropyrazole derivatives, (5), (7) and (8), which have been solved by X-ray crystallography; those of the remaining five compounds were already known. Except for (8), there appears to be an opening of the intramolecular angle at C(4) due to the presence of the nitro group, that, on the other hand, seems to have no correlation with the presence of the hydrogen H(1)/H(2) disorder. Crystal structure diagrams and intermolecular contacts were analysed for either pyrazole derivatives with and without nitro substituents. There appear to be two general modes of packing: the first is based upon a secondary structure of trimers in sheets, which distorts into helices; the second is made of dimers, which then pack into sheets. The nitro group seems to have no influence in the packing, which is more controlled by the substituents at C(3) and C(5). Although only partly successful, we have established some relationships between crystallographic results and thermodynamic properties. First, between the planarity or not of the 4-nitro group and the acid and basic pK_a's, and second, between some packing descriptors and the sublimation enthalpies.

Introduction

We are in the process of carrying out a systematic study of the properties of NH-pyrazoles in the solid state by X-ray crystallography (Llamas-Saiz, Foces-

Acta Crystallographica Section B
ISSN 0108-7681 ©1994

Foces, Elguero & Meutermans, 1992; Foces-Foces, Cano & Elguero, 1993; Foces-Foces, Llamas-Saiz, Claramunt, López & Elguero, 1994; Llamas-Saiz, Foces-Foces & Elguero, 1995), ^{13}C and ^{15}N solid-state CPMAS NMR (Smith *et al.*, 1989; Aguilar-Parrilla, Scherer *et al.*, 1992; Aguilar-Parrilla, Cativiela *et al.*, 1992) and thermochemistry (Colomina, Jiménez & Turrión, 1982; Jiménez, Roux, Turrión & Gomis, 1987; Elguero *et al.*, 1991; Jiménez, Roux & Turrión, 1992). Due to the lack of studies relating these properties of the solid state, it is necessary to compare a set of compounds large enough to have a chance of discovering some general rules. In the present paper, a series of four pyrazole pairs, without and with a 4-nitro substituent, will be examined.

The aims of this study are: (i) to discuss the molecular geometries with special stress on the effect of the nitro group; (ii) to classify the eight pyrazoles (1–8) according to packing patterns, particularly N—H···N hydrogen bonds (secondary structure); (iii) to try empirical relationships between the crystal structure and some thermodynamical properties, such as solution pK_a's and heats of sublimation.

Experimental

Compounds (5)–(8) were prepared according to known procedures; the first three by a nitration of the corresponding pyrazoles (1–3) and the last one by oxidation of 3,5-diphenyl-4-nitropyrazole [nitration of 3,5-diphenylpyrazole (4) leads to nitrophenyl

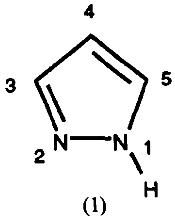

(1)

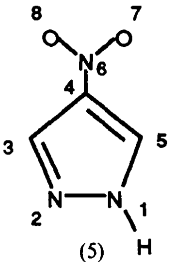

(5)

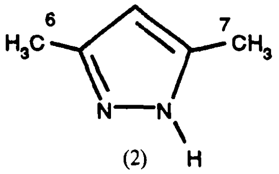

(2)

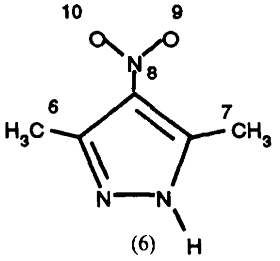

(6)

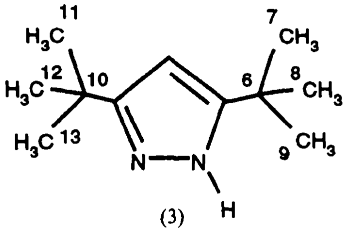

(3)

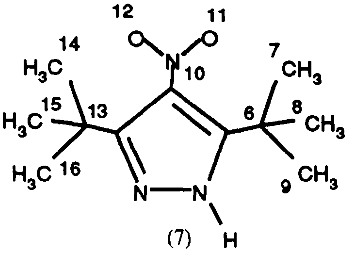

(7)

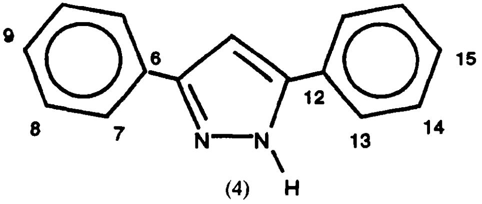

(4)

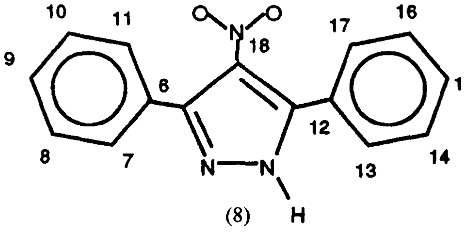

(8)

Table 1. *Vapor pressures*

T (K)	t (s)	Δm (mg)	p (Pa)	$10^2 \times \delta p$ (p)	T (K)	t (s)	Δm (mg)	p (Pa)	$10^2 \times \delta p$ (p)
3,5-Di-*tert*-butylpyrazole (3)									
323.56	14 760	1.72	0.468	+0.503	334.52	12 600	4.64	1.50	+0.558
326.76	12 840	2.10	0.656	−0.526	337.73	11 340	5.74	2.07	+0.0980
329.96	16 500	3.77	0.923	−0.503	340.81	11 220	7.66	2.81	−0.104
332.43	16 260	4.80	1.20	−0.149					
3,5-Diphenylpyrazole (4)									
386.02	27 180	3.28	0.0553	−0.438	395.94	26 880	8.90	0.153	−0.201
389.30	26 580	4.52	0.0782	−0.270	399.39	21 600	10.32	0.223	+2.02
392.50	27 000	6.50	0.111	+1.68	402.78	20 940	13.50	0.302	−0.964
4-Nitropyrazole (5)									
318.60	29 820	2.01	0.0391	+0.360	330.69	18 360	4.57	0.147	−0.542
322.08	22 020	2.17	0.0577	−0.132	333.56	24 420	8.20	0.200	+0.0123
324.56	30 120	3.93	0.0765	+0.507	336.15	18 000	7.94	0.263	+0.558
327.67	24 240	4.41	0.107	+0.0802					
3,5-Dimethyl-4-nitropyrazole (6)									
326.76	21 600	3.25	0.0792	−0.164	337.56	23 940	11.46	0.256	+0.859
329.61	19 440	4.09	0.111	+2.18	340.63	17 713	11.31	0.343	−1.59
331.74	20 280	5.12	0.134	−2.12	343.41	11 580	9.74	0.454	−1.78
334.68	19 380	6.96	0.191	+1.86	347.34	18 180	23.39	0.698	+2.10
3,5-Di-*tert*-butyl-4-nitropyrazole (7)									
340.63	24 600	3.72	0.0644	+0.822	353.35	25 680	15.31	0.258	+0.182
344.18	21 960	4.84	0.0943	−0.987	356.43	20 640	16.82	0.355	−0.165
347.39	29 580	9.50	0.138	+1.68	359.47	19 200	21.41	0.487	+0.148
350.31	24 900	10.78	0.187	+0.398					
3,5-Diphenyl-4-nitropyrazole (8)									
407.34	26 580	2.29	0.0370	−0.451	422.05	18 480	7.69	0.182	+1.40
410.60	23 880	2.98	0.0538	+0.932	424.64	26 400	14.34	0.238	+1.64
421.38	26 700	3.07	0.0658	+1.92	428.06	18 300	13.87	0.333	+1.10
416.45	27 120	6.21	0.0993	−0.556	431.27	16 560	17.06	0.454	−0.414
418.86	26 040	7.58	0.127	−1.37					

Table 2. *Molar enthalpies of sublimation*

Compound	θ (K)	A	B	$\Delta_{sub}H_m$ (θ) (kJ mol^{-1})	$\Delta_{sub}H^0_m$(298.15 K) (kJ mol^{-1})	T (0.5 Pa) (K)	$\Delta_{sub}H^0_m$($T_{0.5\text{ Pa}}$) (kJ mol^{-1})
Pyrazole (1)	275.43	14.32 ± 0.07	−3882.5 ± 19.2	74.3 ± 0.4	74.0 ± 0.4*	265.54	74.7†
3.5-Dimethylpyrazole (2)	300.92	14.64 ± 0.03	−4350.9 ± 8.9	83.3 ± 0.2	83.3 ± 0.2‡	291.20	83.7†
3,5-Di-*tert*-butylpyrazole (3)	332.19	15.10 ± 0.05	−4993.2 ± 15.4	95.6 ± 0.3	96.8 ± 0.3	324.21	95.9§
3,5-Diphenylpyrazole (4)	394.40	16.52 ± 0.17	−6861.0 ± 68.1	131.4 ± 1.3	135.1 ± 1.3	407.88	130.8§
4-Nitropyrazole (5)	327.38	14.43 ± 0.04	−5046.2 ± 13.6	96.6 ± 0.3	97.4 ± 0.3	342.56	96.1§
3,5-Dimethyl-4-nitropyrazole (6)	337.05	14.69 ± 0.15	−5158.5 ± 52.1	98.8 ± 1.0	99.9 ± 1.0	344.11	98.6§
3,5-Di-*tert*-butyl-4-nitropyrazole (7)	350.05	15.63 ± 0.09	−5729.5 ± 31.3	109.7 ± 0.6	114.4 ± 0.6	359.64	109.0§
3,5-Diphenyl-4-nitropyrazole (8)	419.31	18.19 ± 0.11	−7992.2 ± 44.9	153.0 ± 0.9	160.2 ± 0.9	432.22	159.3§

* Jiménez, Roux, Turrión & Gomis (1987).

† Estimated assuming a variation of the sublimation enthalpy of 0.04 per K.

‡ Elguero *et al.* (1991).

§ Determined from the sublimation enthalpies at θ temperature and from the values of C_p in the condensed phase determined in our laboratory by DSC and the values of C_p in the gas phase calculated with the group contributions of Rihani & Donaiswamy (1965).

derivatives: (5) (Hüttel, Büchele & Jochum, 1955), (6) (Elguero, Jacquier & Tien Duc, 1966), (7) (Habraken, Beenaker & Brussee, 1972) and (8) (Hüttel, Büchele & Jochum, 1955; Babar, Desai & Shinde, 1983)].

Enthalpies of sublimation

The enthalpies of sublimation of (3)–(8) were obtained from vapor pressures determined by the Knudsen effusion method, using a technique and procedure previously described (Colomina, Jiménez & Turrión, 1982; Elguero *et al.*, 1991). The details of the two orifices employed were as follows: orifice area $(7.99 \pm 0.03) \times 10^{-4}$ cm^2 and Clausing coefficient $W_a = 0.958 \pm 0.009$ for 3,5-di-*tert*-butylpyrazole; orifice areas $(0.69 \pm 0.01) \times 10^{-3}$ cm^2 and Clausing coefficient $W_a = 0.986 \pm 0.003$ for the remaining compounds. The results of the Knudsen effusion experiments are summarized in Table 1, in which values of temperature, time and mass of sublimed substance are collected, an equation of the type $lg(p/\text{Pa}) = -B(T/K)^{-1} + A$ was fitted to the results of Table 1 by a least-squares method. The

Table 3. *Crystal analysis parameters at room temperature*

	(5)	(7)	(8)
Crystal data			
Formula	$C_3H_4N_3O_2$	$C_{11}H_{19}N_3O_2$	$C_{15}H_{11}N_3O_2$
Crystal habit	Colorless needle	Yellow plate	Colorless prism
Crystal size (mm)	0.12 × 0.05 × 0.05	0.33 × 0.33 × 0.03	0.30 × 0.17 × 0.10
Symmetry	Triclinic, $P\bar{1}$	Monoclinic, $P2_1/c$	Monoclinic, $P2_1/c$
Unit-cell determination:	Least-squares fit from 66 reflections ($\theta < 45°$)	Least-squares fit from 78 reflections ($\theta < 45°$)	Least-squares fit from 71 reflections ($\theta < 45°$)
Unit-cell dimensions			
a (Å)	9.8831 (7)	10.6407 (4)	18.1399 (16)
b (Å)	9.6688 (7)	9.6180 (4)	12.0814 (9)
c (Å)	8.3417 (4)	12.6649 (5)	11.5184 (7)
α (°)	81.139 (4)	90	90
β (°)	100.076 (4)	107.962 (3)	99.339 (7)
γ (°)	105.966 (6)	90	90
Packing: V (Å^3), Z	749.8 (1), 6	1233.0 (1), 4	2490.9 (3), 8
D_c (g cm^{-3}), M, $F(000)$	1.503, 113.08, 348	1.214, 225.29, 488	1.415, 265.27, 1104
μ (cm^{-1})	10.71	6.56	7.56
Experimental data			
Technique	Four circle diffractometer: Philips PW1100, bisecting geometry Graphite-oriented monochromator: Cu $K\alpha$ $\omega/2\theta$ scans, scan width: 1.5° Detector apertures 1 × 1°; 1 min/reflex, θ_{max} = 65°		
Number of reflections			
Independent	2217	2101	4231
Observed	1737 [$3\sigma(I)$ criterion]	1778 [$3\sigma(I)$ criterion]	2380 [$3\sigma(I)$ criterion]
Range:			
h	0→10	0→11	0→21
k	−10→10	0→11	0→13
l	−9→9	−14→14	−13→13
Standard reflections	2 reflections every 90 min; no variation		
Solution and refinement			
Solution	*SIR*88	*SIR*88	*SIR*88 + *DIRDIF*
Refinement:			
Least-squares on F_o	Full-matrix	Full-matrix	Two blocks
Parameters:			
Number of variables	265*	221	494*
Degrees of freedom	1472	1557	1886
Ratio of freedom	6.6	8.0	4.8
H atoms	From difference synthesis		
Final shift/error	0.05	0.02	0.16
Weighting scheme	Empirical as to give no trends in $\langle w\Delta^2F\rangle$ *versus* $\langle\lvert F_{obs}\rvert\rangle$ and $\langle\sin\theta/\lambda\rangle$		
Max. thermal value (Å^2)	$U_{22}[O(8A)] = 0.166$ (3)	$U_{33}[O(11)] = 0.117$ (2)	$U_{22}[C(303)] = 0.21$ (1)
Final $\Delta\rho$ (e Å^{-3})	± 0.33	± 0.20	± 0.42
Final R and wR	0.063, 0.071	0.049, 0.051	0.082, 0.087
S	1.12	1.03	0.95

* See text.

coefficients A and B of the equations concerning the studied compounds are shown in Table 2. The enthalpies of sublimation of the compounds, corresponding to the mean temperature θ of its experimental range, have been calculated from the corresponding B values and are also collected in Table 2. The uncertainties assigned to the values of ΔH^0_{sub} are based on the standard deviations of B values. The values for the enthalpies of sublimation 298.15 K have been computed from the $C^0_{p,m}$ (*cr*) values determined by DSC and $C^0_{p,m}$ (*g*) values calculated using the group-contribution scheme of Rihani & Donaiswamy (1965). Control of purity, assessed by DSC using the fractional-fusion technique (Martí, 1973) indicated that the mole fraction of impurities of (3), (4), (6) and (7) was less than 0.001. The method cannot be used for compounds (5) and (8), since they decompose on melting.

X-ray structure determination. Table 3 contains the crystal data and refinement parameters for (5), (7) and (8). The structures were solved by direct methods and refined by least-squares procedures. The calculations were performed on a VAX6410 computer using the following set of programs: *SIR*88 (Burla *et al.*, 1989), *DIRDIF* (Beurskens *et al.*, 1984), *XRAY*80 system (Stewart *et al.*, 1976), *XTAL*3.2 (Hall, Flack & Stewart, 1993), *PESOS* (Martinez-Ripoll & Cano, unpublished) and *PARST* (Nardelli, 1983). The metric of (5) is obviously pseudo-rhombohedric; proofs on the symmetry rejected the possibility of a rhombohedral cell, the slight variations being enough to keep this structure as triclinic. The structure of (8) was solved in the $P2_1$ space group, but the four independent molecules obtained in this way did not refine properly. The molecules were related in pairs by symmetry centers, but its relative position was incompatible with other space groups of higher symmetry. The correct solution was found in $P2_1/c$, with one 'complete' molecule and two halves related by a pseudo-symmetry center at $(\frac{1}{2},0,\frac{1}{4})$ in the asymmetric unit. Each of these half molecules generates a model of disorder through a crystallographic symmetry center. The atomic scattering factors were taken from *International Tables for X-ray Crystallography* (1974, Vol. IV). Fractional atomic coordinates for (5), (7) and (8) are given in Tables 4–6.*

Results and discussion

Thermodynamics

The values of $\Delta_{\text{vap}}H^0$ (in kJ mol^{-1}) for benzene 33.8 (Osborne & Ginnings, 1947), toluene 38.0 (Scott *et al.*, 1962), *tert*-butylbenzene 48.1 (Prosen, Johnson & Rossini, 1946), phenylbenzene (biphenyl) 81.8 (Montgomery & Rossini, 1978) and nitrobenzene 56.1 (Lebedeva, Katin & Akhemedora, 1971) have been reported. Since we have a collection of aromatic compounds (mono-substituted benzenes and disubstituted pyrazoles) with the same series of substituents, we have represented in Fig. 1. the differences in sublimation enthalpies of pyrazoles [$\delta\Delta_{\text{sub}}H^0 = \Delta_{\text{sub}}H^0_{\text{disubstituted pyrazole}} - \Delta_{\text{sub}}H^2_{\text{parent pyrazole}}$] against those of benzenes [$\delta\Delta_{\text{vap}}H^0 = 2 \times (\Delta_{\text{vap}}H^0_{\text{monosubstituted benzene}} - \Delta_{\text{vap}}H^0_{\text{benzene itself}})$]. For instance, for the methyl group, $\Delta_{\text{vap}}H^0_{\text{toluene}} = 38.0$, $\Delta_{\text{vap}}H^0_{\text{benzene}} = 33.8$, $\delta\Delta_{\text{vap}}H^0 = 2 \times (38.0 - 33.8) = 8.4$ kJ mol^{-1} (in this case the experimental value for the disubstituted benzene is known and the additivity can be tested, *m*-xylene, $\Delta_{\text{vap}}H^0 = 42.7$, *i.e.* $\delta\Delta_{\text{vap}}H^0 = 8.9$ kJ mol^{-1}). The reasoning behind Fig. 1 assumes that there is a direct relationship between enthalpies of sublimation and enthalpies of vaporization, *i.e.* that enthalpies of melting are constant or proportional to the enthalpies of vaporization. Although the model is rather rough, the result is surprisingly good, and some small deviations are noted that we will try to explain based on crystallographic evidence (see 'Relationships between crystallography and thermodynamic properties').

X-ray crystallography

Molecular structure. The structures of the following pyrazoles have been published: (1) (LaTour & Rasmussen, 1973), (2) (Smith *et al.*, 1989) (3) (Aguilar-Parrilla, Limbach, Foces-Foces, Cano & Elguero, 1994), (4) (Aguilar-Parrilla, Scherer *et al.*, 1992) and (6) (Foces-Foces, Cano & Elguero, 1993). Selected geometrical parameters for (5)–(8) are given in Table 7 [the geometry of the disordered molecules of (8) is omitted].

Table 4. *Final atomic coordinates and* U_{eq} *for* (5)

$$U_{\text{eq}} = (1/3)\Sigma[U_{ij}a_i^*a_j^*a_ia_j\cos(\mathbf{a}_i.\mathbf{a}_j)] \times 10^3.$$

	x	y	z	U_{eq}
N(1*A*)	0.0375 (3)	0.3279 (3)	−0.0574 (4)	53 (1)
N(2*A*)	0.1002 (3)	0.4612 (3)	−0.1237 (3)	52 (1)
C(3*A*)	0.0139 (3)	0.5006 (3)	−0.2498 (4)	53 (1)
C(4*A*)	−0.1074 (3)	0.3895 (3)	−0.2653 (3)	47 (1)
C(5*A*)	−0.0887 (3)	0.2832 (3)	−0.1425 (4)	52 (1)
N(6*A*)	−0.2303 (3)	0.3848 (4)	−0.3837 (4)	70 (1)
O(7*A*)	−0.3288 (3)	0.2741 (4)	−0.3770 (4)	99 (2)
O(8*A*)	−0.2322 (4)	0.4897 (5)	−0.4850 (4)	114 (2)
N(1*B*)	0.3096 (3)	0.2559 (3)	0.2909 (3)	53 (1)
N(2*B*)	0.1740 (3)	0.1941 (3)	0.2316 (3)	54 (1)
C(3*B*)	0.1318 (3)	0.0688 (3)	0.3199 (4)	53 (1)
C(4*B*)	0.2420 (3)	0.0490 (3)	0.4374 (3)	46 (1)
C(5*B*)	0.3532 (3)	0.1702 (3)	0.4151 (4)	54 (1)
N(6*B*)	0.2441 (4)	−0.0686 (3)	0.5593 (4)	64 (1)
O(7*B*)	0.3543 (4)	−0.0673 (4)	0.6540 (4)	95 (1)
O(8*B*)	0.1340 (4)	−0.1671 (3)	0.5638 (4)	96 (1)
N(1*C*)	0.3742 (3)	0.6109 (3)	0.0312 (3)	50 (1)
N(2*C*)	0.4432 (3)	0.5436 (3)	0.1582 (3)	49 (1)
C(3*C*)	0.5695 (3)	0.6305 (3)	0.2011 (4)	50 (1)
C(4*C*)	0.5803 (3)	0.7566 (3)	0.0968 (4)	45 (1)
C(5*C*)	0.4547 (3)	0.7403 (3)	−0.0085 (4)	51 (1)
N(6*C*)	0.6989 (3)	0.8796 (3)	0.0952 (4)	67 (1)
O(7*C*)	0.6886 (4)	0.9823 (3)	−0.0079 (5)	99 (1)
O(8*C*)	0.8028 (3)	0.8753 (4)	0.1975 (5)	101 (2)

Table 5. *Final atomic coordinates and* U_{eq} *for* (7)

$$U_{\text{eq}} = (1/3)\Sigma[U_{ij}a_i^*a_j^*a_ia_j\cos(\mathbf{a}_i.\mathbf{a}_j)] \times 10^4.$$

	x	y	z	U_{eq}
N(1)	0.3863 (1)	0.3877 (2)	0.4378 (1)	352 (4)
N(2)	0.5104 (1)	0.3429 (1)	0.4467 (1)	364 (4)
C(3)	0.4965 (1)	0.2322 (2)	0.3811 (1)	309 (5)
C(4)	0.3595 (2)	0.2093 (2)	0.3316 (1)	315 (5)
C(5)	0.2909 (1)	0.3095 (2)	0.3707 (1)	312 (5)
C(6)	0.1450 (1)	0.3389 (2)	0.3513 (1)	367 (5)
C(7)	0.0882 (2)	0.2282 (3)	0.4106 (2)	604 (9)
C(8)	0.0709 (2)	0.3398 (2)	0.2262 (2)	520 (7)
C(9)	0.1282 (2)	0.4814 (2)	0.3988 (2)	465 (6)
N(10)	0.3010 (1)	0.1057 (2)	0.2493 (1)	426 (5)
O(11)	0.2098 (2)	0.0360 (2)	0.2595 (2)	751 (7)
O(12)	0.3442 (2)	0.0922 (2)	0.1714 (1)	730 (7)
C(13)	0.6162 (2)	0.1499 (2)	0.3752 (1)	369 (5)
C(14)	0.6528 (3)	0.1934 (3)	0.2719 (2)	597 (9)
C(15)	0.7330 (2)	0.1797 (3)	0.4780 (2)	659 (9)
C(16)	0.5889 (2)	−0.0064 (2)	0.3710 (2)	538 (8)

The only significant difference amongst the three independent molecules of (5) is the C(4)—C(5) bond distance of molecules *A* and *B*, as tested by half-normal probability plots (Abrahams & Keve, 1971). Their pyrazole rings do not deviate significantly from planarity (χ^2 in the range 0.25–0.86 *versus* the tabulated value of 5.99). The presence of bulky substituents (*tert*-butyl or phenyl groups) in positions 3 and 5 causes the loss of planarity of the pyrazole ring [$\chi^2 = 83.17$ and 49.72 in (7) and (8)]. The increase of the torsion angles of the phenyl rings when (4) and (8) are compared is related to the esteric and electronic effects of the nitro group (see below).

---

* Lists of structure factors, anisotropic displacement parameters, H-atoms parameters, complete geometry, torsion angles and least-squares planes data have been deposited with the IUCr (Reference: HE0089). Copies may be obtained through The Managing Editor, International Union of Crystallography, 5 Abbey Square, Chester CH1 2HU, England.

Table 6. *Final atomic coordinates and* U_{eq} *for* (8)

$U_{eq} = (1/3)\Sigma[U_{ij}a_i^*a_j^*a_ia_j\cos(\mathbf{a}_i.\mathbf{a}_j)] \times 10^3$.

	x	y	z	U_{eq}
N(101)	0.0111 (3)	0.3725 (3)	0.0517 (4)	56 (2)
N(102)	−0.0402 (3)	0.3818 (4)	−0.0467 (4)	60 (2)
C(103)	−0.0418 (3)	0.2831 (4)	−0.0997 (4)	41 (1)
C(104)	0.0109 (3)	0.2113 (3)	−0.0289 (4)	37 (1)
C(105)	0.0453 (3)	0.2778 (3)	0.0660 (4)	40 (1)
C(106)	−0.0964 (3)	0.2565 (4)	−0.2057 (4)	44 (2)
C(107)	−0.1084 (3)	0.3375 (5)	−0.2933 (5)	53 (2)
C(108)	−0.1619 (3)	0.3216 (5)	−0.3903 (5)	53 (2)
C(109)	−0.2043 (4)	0.2283 (5)	−0.3986 (5)	63 (2)
C(110)	−0.1956 (3)	0.1562 (5)	−0.3165 (5)	53 (2)
C(111)	−0.1432 (3)	0.1597 (4)	−0.2106 (5)	48 (2)
C(112)	0.1017 (2)	0.2586 (4)	0.1720 (4)	42 (1)
C(113)	0.1004 (3)	0.1606 (4)	0.2393 (4)	47 (2)
C(114)	0.1502 (3)	0.1550 (5)	0.3457 (5)	53 (2)
C(115)	0.1981 (4)	0.2407 (7)	0.3825 (6)	75 (3)
C(116)	0.2002 (3)	0.3271 (5)	0.3203 (5)	53 (2)
C(117)	0.1539 (3)	0.3443 (4)	0.2051 (5)	46 (2)
N(118)	0.0361 (2)	0.1101 (3)	−0.0624 (3)	39 (1)
O(119)	0.0122 (2)	0.0734 (3)	−0.1637 (4)	61 (1)
O(120)	0.0839 (3)	0.0577 (3)	0.0048 (4)	66 (1)
N(201)	0.5108 (6)	−0.1203 (7)	0.5521 (9)	56 (3)
N(202)	0.4575 (5)	−0.1257 (6)	0.4525 (7)	46 (3)
C(203)	0.4565 (3)	−0.0041 (7)	0.4183 (5)	69 (2)
C(204)	0.5123 (5)	0.0380 (7)	0.4714 (8)	35 (3)
C(206)	0.4007 (3)	−0.0049 (4)	0.3115 (5)	44 (2)
C(207)	0.3918 (3)	−0.0902 (5)	0.2309 (7)	68 (2)
C(208)	0.3392 (5)	−0.0823 (9)	0.1313 (8)	99 (4)
C(209)	0.2943 (4)	0.0066 (7)	0.1073 (5)	70 (3)
C(210)	0.3031 (4)	0.1010 (5)	0.1894 (5)	60 (2)
C(211)	0.3579 (3)	0.0868 (4)	0.2819 (4)	44 (2)
N(218)	0.5405 (5)	0.1438 (6)	0.4327 (7)	38 (3)
O(219)	0.5157 (4)	0.1749 (5)	0.3359 (6)	46 (2)
O(220)	0.5878 (4)	0.1923 (5)	0.5025 (6)	52 (2)
N(301)	0.4803 (5)	−0.1267 (7)	−0.0472 (9)	53 (3)
N(302)	0.5367 (5)	−0.1325 (6)	0.0513 (7)	48 (3)
C(303)	0.5435 (4)	−0.0048 (10)	0.0807 (6)	107 (4)
C(304)	0.4882 (5)	0.0350 (6)	0.0263 (8)	33 (3)
C(306)	0.6000 (3)	−0.0072 (4)	0.1884 (5)	51 (2)
C(307)	0.6468 (4)	0.0783 (4)	0.2113 (5)	55 (2)
C(308)	0.7031 (3)	0.0922 (5)	0.3034 (5)	57 (2)
C(309)	0.7064 (3)	0.0027 (6)	0.3907 (5)	62 (2)
C(310)	0.6551 (4)	−0.0835 (7)	0.3704 (8)	86 (3)
C(311)	0.6044 (3)	−0.0885 (5)	0.2714 (7)	68 (2)
N(318)	0.4651 (6)	0.1429 (6)	0.0625 (9)	111 (4)
O(319)	0.4898 (4)	0.1761 (5)	0.1610 (6)	48 (2)
O(320)	0.4170 (5)	0.1945 (5)	−0.0070 (6)	54 (2)

The *tert*-butyl substituent closes the angles at C(3) and C(5) in (3) with respect to the pyrazole itself (1) (La Tour & Rasmussen, 1973). The opening of the angle at C(4) due to the nitro group (see below) increases, in (7), the effect of the *tert*-butyl group at C(3) and C(5) (Table 7). The methyl and phenyl groups in the series (1, 2, 6) and (1, 4, 8) follow the same tendency, considering the mean values of angles at C(3) and C(5) [the averaging is necessary in the case of pyrazoles with disordered N—H hydrogen, since this disorder symmetrizes the pyrazole ring in compounds (5) and (6)]. In 3,5-dimethylpyrazole (2) and its corresponding nitro derivative (6), only one half of the molecule is crystallographically independent.

There is no relationship between the presence or absence of the nitro group and the hydrogen disorder of N—H. All possible combinations H-ordered/H-disordered are present in the four pairs of compounds (1–5, ... 4–8). When the H atom is localized at N(1) it is involved in hydrogen bonds with the nitro group.

The influence of a 4-*nitro group on the geometry of pyrazoles.* To discuss this point, we will follow the same procedure that we have already used for *N*-substituted pyrazoles (Llamas-Saiz, Foces-Foces & Elguero, 1995). In order to differentiate between intrinsic effects, that is, effects which are characteristic of the isolated molecule, and crystal packing effects, high-level *ab initio* calculations are necessary to determine the geometry of the isolated molecule. According to Pople (Hehre, Radom, Schleyer & Pople, 1986), 6-31*G***//6-31*G*** calculations provide good-to-excellent molecular geometries.

Using the *Gaussian*92 series of programs (Frisch *et al.*, 1992), the geometry of 4-nitropyrazole (5) planar and perpendicular (φ = 0 and 90°) was calculated (Table 8). Nitrobenzene, with the same conformation, was also calculated for comparative purposes. The nitrobenzene geometries were identical to those obtained at the 6-31*G**//6-31*G** level (Ritchie, 1988). The most characteristic effects of the nitro group in benzenes are the angular deformations; in crystals these deformations amount to 2.9 (2), −1.9 (1), 0.3 (1) and 0.4 (2)° for C_{ipso}, C_{ortho}, C_{meta} and C_{para}, respectively (Domenicano & Murray-Rust, 1979). The corresponding 6-31*G*** values (Table 8) are 2.4, −1.5, 0.1 and 0.5° [the underestimation of ΔC_{ipso} has already been noticed (Ritchie, 1988)].

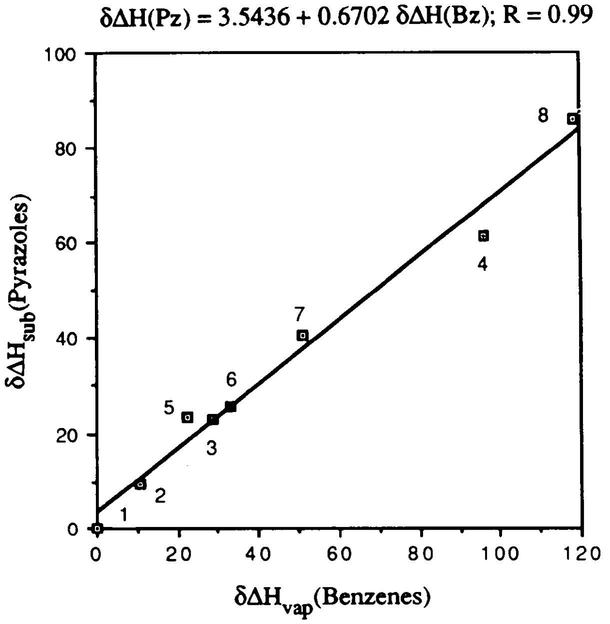

Fig. 1. Plot of $\delta\Delta H_{sub}$(pyrazoles) *versus* $\delta\Delta H_{vap}$(benzenes) (all values in kJ mol^{-1}).

Table 7. *Geometrical parameters for* (5)–(8)

The numbering system is not necessarily coincident with that used in the crystallographic work [only the geometry of the ordered molecule in (8) has been included].

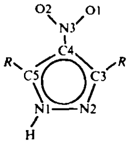

	(5), $R = H$			(6), $R = CH_3$	(7), $R = C(CH_3)_3$	(8), $R = C_6H_6$
N(1)—N(2)	1.345 (3)	1.348 (3)	1.339 (4)	1.339 (11)	1.361 (2)	1.350 (6)
N(2)—C(3)	1.312 (4)	1.318 (4)	1.323 (4)	1.318 (12)	1.329 (2)	1.339 (6)
C(3)—C(4)	1.374 (4)	1.367 (4)	1.375 (4)	1.388 (13)	1.415 (2)	1.443 (6)
C(4)—C(5)	1.362 (4)	1.382 (4)	1.375 (4)	1.388 (13)	1.389 (2)	1.417 (6)
C(5)—N(1)	1.317 (4)	1.312 (4)	1.314 (4)	1.318 (12)	1.337 (2)	1.299 (6)
C(3)—*R*	—	—	—	1.502 (13)	1.523 (2)	1.477 (6)
C(5)—*R*	—	—	—	1.502 (13)	1.522 (2)	1.479 (6)
C(4)—N(3)	1.420 (4)	1.407 (4)	1.422 (4)	1.412 (17)	1.437 (2)	1.382 (6)
N(3)—O(1)	1.217 (5)	1.235 (4)	1.221 (4)	1.209 (15)	1.218 (3)	1.257 (5)
N(3)—O(2)	1.235 (4)	1.226 (5)	1.224 (4)	1.209 (15)	1.219 (3)	1.239 (5)
C(5)—N(1)—N(2)	108.8 (3)	109.2 (3)	109.4 (3)	109.8 (8)	113.6 (1)	115.4 (4)
N(1)—N(2)—C(3)	108.9 (3)	108.5 (3)	109.0 (3)	109.8 (8)	106.5 (1)	105.7 (4)
N(2)—C(3)—C(4)	107.8 (3)	108.4 (3)	107.3 (3)	106.7 (7)	107.7 (1)	108.3 (4)
C(3)—C(4)—C(5)	106.6 (3)	106.2 (3)	106.7 (3)	107.0 (6)	108.4 (1)	105.3 (4)
C(4)—C(5)—N(1)	108.0 (3)	107.8 (3)	107.5 (3)	106.7 (7)	103.8 (1)	105.1 (4)
N(2)—C(3)—*R*	—	—	—	121.7 (9)	120.9 (1)	122.2 (4)
C(4)—C(3)—*R*	—	—	—	131.7 (10)	131.3 (1)	129.1 (4)
N(1)—C(5)—*R*	—	—	—	121.7 (9)	122.2 (3)	119.7 (4)
C(4)—C(5)—*R*	—	—	—	131.7 (10)	133.9 (1)	135.0 (4)
C(3)—C(4)—N(3)	127.5 (3)	127.9 (3)	127.0 (3)	126.5 (4)	126.0 (2)	126.3 (4)
C(5)—C(4)—N(3)	125.9 (3)	126.0 (3)	126.3 (3)	126.5 (4)	125.5 (1)	126.4 (4)
C(4)—N(3)—O(1)	118.3 (4)	117.5 (3)	117.5 (3)	118.1 (6)	118.3 (2)	119.4 (4)
C(4)—N(3)—O(2)	117.6 (3)	118.3 (3)	117.5 (3)	118.1 (6)	119.1 (2)	120.4 (4)
O(1)—N(3)—O(2)	124.2 (4)	124.2 (3)	125.0 (3)	123.8 (9)	122.6 (2)	120.1 (4)
C(3)—C(4)—N(3)—O(1)	−0.2 (6)	−0.3 (5)	−0.7 (5)	−2.4 (13)	−45.7 (3)	−0.2 (6)
N(2)—C(3)—C—C	—	—	—	—	20.0 (2)	43.9 (7)
N(1)—C(5)—C—C	—	—	—	—	11.5 (2)	−44.8 (7)

For (1)–(4): N(2)—C(3)—C(4) = 112.3 (5), 107.8 (8), 109.9 (4) and 107.9 (3)°; C(3)—C(4)—C(5) = 105.0 (5), 103.6 (6), 105.8 (4) and 106.3 (3)°; N(1)—C(5)—C(4) = 106.6 (5), 107.8 (8), 106.7 (4) and 107.8 (3)°, respectively. The N(2)—C(3)—C—C/N(1)—C(5)—C—C angles are 18.8 (5)/ −7.3 (5)° and −15.7 (5)/35.7 (6)° for the two independent molecules in (4), while in (3), the *tert*-butyl groups are twisted by −52.9 (8) and [47.0 (14), −1.6 (9)°], the latter being disordered.

Torsion of the nitro group in nitrobenzene has little influence on the benzene geometry [the C(1)—N(3) bond length is increased by 0.005 Å], although resonance interaction is lost in the $\varphi = 90°$ conformation. The situation in 4-nitropyrazoles is different, since pyrazoles are π-electron-rich compounds (Elguero, 1984) and, consequently, charged resonance forms like (5*b*) are more important than the corresponding resonance form in nitrobenzene.

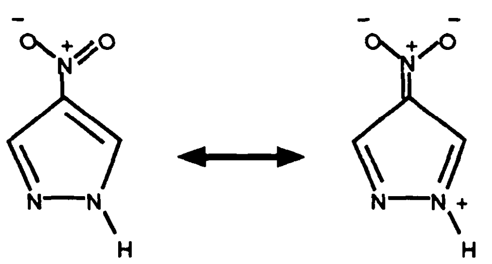

(5*a*) (5*b*)

The calculated geometry for 4-nitropyrazole $\varphi = 0°$, which corresponds to the energy minimum, is in excellent agreement with the average experimental geometry of (5) (Table 7). This shows that packing effects can be neglected in a first approximation. The calculated effect of the nitro group on the C(3)—C(4)—C(5) angle is 2.1°, a little smaller than in benzene, but a pentagon is more difficult to deform than a hexagon. The experimental effect depends on pyrazole pairs (when several independent molecules are present in the unit cell the average value has been calculated): (5) (106.5°)–(1) (104.4°) = 2.1°, (6) (107.0°)–(2) (106.3°) = 0.7°, (7) (108.4°)–(3) (105.8°) = 2.6° and (8) (105.3°)–(4) (106.7°) = −1.4°. For pyrazole itself, pair (1, 5), the *ab initio* calculated and the crystallographically determined differences coincide (2.1°). For 3,5-di-*tert*-butylpyrazole, pair (3, 7), the value of 2.6° is consistent, taking into account the non-neglible effect of two *tert*-butyl groups. For 3,5-dimethylpyrazole, pair (2, 6), the effect, 0.7°, is

Table 8. *Geometrical parameters resulting from a HF*/6-31*G*** *calculation of* 4-*nitropyrazole* (5) *and nitrobenzene*

Geometry	Pyrazole (1)*	4-Nitropyrazole ($\varphi = 0^\circ$)†	4-Nitropyrazole ($\varphi = 90^\circ$)‡	Geometry	Nitrobenzene ($\varphi = 0^\circ$)§	Nitrobenzene ($\varphi = 90^\circ$)¶
N(1)—N(2)	1.330	1.340	1.327	C(1)—C(2)	1.383	1.378
N(2)—C(3)	1.302	1.296	1.300	C(2)—C(3)	1.383	1.385
C(3)—C(4)	1.413	1.410	1.406	C(3)—C(4)	1.386	1.386
C(4)—C(5)	1.363	1.366	1.357	C(4)—C(5)	1.386	1.386
C(5)—N(1)	1.341	1.327	1.338	C(5)—C(6)	1.383	1.385
C(4)—N(3)	—	1.419	1.447	C(6)—C(1)	1.383	1.378
N(3)—O(1)	—	1.192	1.192	C(1)—N(3)	1.459	1.464
N(3)—O(2)	—	1.192	1.192	N(3)—O(1)	1.194	1.192
C(5)—N(1)—N(2)	112.79	113.52	113.29	C(2)—C(1)—C(6)	122.36	122.94
N(1)—N(2)—C(3)	104.99	105.56	105.72	C(3)—C(2)—C(1)	118.48	118.18
N(2)—C(3)—C(4)	111.68	109.93	109.87	C(4)—C(3)—C(2)	120.10	120.19
C(3)—C(4)—C(5)	103.91	105.97	106.10	C(5)—C(4)—C(3)	120.48	120.32
C(4)—C(5)—N(1)	106.63	105.01	105.02	C(4)—C(5)—C(6)	120.10	120.19
C(5)—C(4)—N(3)	—	126.11	126.74	C(5)—C(6)—N(1)	118.48	118.18
C(4)—N(3)—O(1)	—	117.41	117.23	C(2)—C(1)—N(3)	118.82	118.53
C(4)—N(3)—O(2)	—	117.30	117.23	C(1)—N(3)—O(1)	117.70	117.13
O(1)—N(3)—O(2)	—	125.29	125.53	O(1)—N(3)—O(2)	124.60	125.74
C(3)—C(4)—N(3)—O(1)	—	0.00	90.00	C(2)—C(1)—N(3)—O(1)	0.00	90.00

* From Llamas-Saiz, Foces-Foces & Elguero (1995).

† $E = -428.2724$ hartrees.

‡ $E = -428.2552$ hartrees.

§ $E = -434.1843$ hartrees; nitrobenzene from CSD: C(2)—C(1)—C(6) = 122.9°, C(3)—C(2)—C(1) = 118.1°, C(4)—C(3)—C(2) = 120.3°, C(5)—C(4)—C(3) = 120.4°.

¶ $E = -434.1722$ hartrees.

too small, maybe due to the fact that these compounds show proton disorder which affects the uncertainty of the difference (Smith *et al.*, 1989; Foces-Foces, Cano & Elguero, 1993). Finally, the value for (8) (105.3°) is abnormally low; this compound with its very short C(4)—N(3) bond length (1.382 Å) and its very long N(3)—O(1,2) bond length (1.248 Å) behaves as a pyrazole with an exaggerated mesomeric effect [as if resonance form (5*b*) would be more important than that in 4-nitropyrazole itself]. This could be related to the small value of the C(3)—C(4)—C(5) angle and with the angular torsion of the phenyl substituents. Other nitropyrazoles, like the pair of tautomers of 3,5-methyl-4-nitropyrazole (Foces-Foces, Llamas-Saiz, Claramunt, López & Elguero, 1994), show C(3)—C(4)—C(5) angles similar to those of (5) and (6).

The torsion of the nitro group produces modifications of the calculated geometry of 4-nitropyrazole. Comparing the $\varphi = 0^\circ$ and $\varphi = 90^\circ$ geometrical parameters of Table 8, some differences can be noted, the most significant being the expected lengthening of the C(4)—N(3) bond, +0.028 Å, due to the suppression of the resonance interaction. The effect is 5.6 times larger than in nitrobenzene. Assuming a $\sin^2\varphi$ variation, the experimental and calculated value for $\varphi = 0^\circ$ (ΔR[C(4)—N(3)] = 0 Å), the calculated value for $\varphi = 90^\circ$ ($\Delta R = 0.028$ Å) and the experimental value for $\varphi = 45.7^\circ$ [(7–5), $\Delta R = 0.011$ Å] are related by $\Delta R\,(\text{Å}) = -0.001 + 0.028\sin^2\varphi$, $r^2 = 0.98$.

Crystal packing

The packing of the eight structures could be classified into two main general modes. The first is present in (1), (2), (5) and (6) and the second in the rest of the structures, (3), (4), (7) and (8), see Figs. 2–9. Tables 9 and 10 describe the main interactions involved in the packings, including the hydrogen bonds, according to the numbering system given in the Introduction. We will describe the packing in terms of structural levels: atoms form molecules (primary structure, 1*ry S*), molecules interact strongly to produce groups (through, for example, hydrogen bonds) of molecules, which form the secondary structure (2*ry S*); these groups associate in motifs through less strong, yet directional forces (tertiary structure, 3*ry S*), which give rise to the crystal (quaternary structure, 4*ry S*) by means of weaker and isotropic interactions; some levels may be absent.

The first model mentioned is based upon the symmetrical packing presented by structure (2) (Fig. 2), the others being viewed as deformations of this. The secondary structure, built by the strongest interactions, is formed by trimers through hydrogen bonds involving the disordered H atoms; the next step in the packing (3*ry S*) is due to H···H contacts between trimers to form sheets perpendicular to the *c*-axis; the sheets are compacted, one with each other, to give the crystal (4*ry S*) by H···ring interactions (see Table 8) and an intersheet distance of 3.499 Å.

Table 9. *Main interactions building the packing in the structures of* (1), (2), (5) *and* (6), *showing the symmetry involved in the interaction and, in parentheses, the corresponding structural level*

Π represents the centroid of the indicated ring. C_k is the packing coefficient as measured by the ratio: van der Waals' molecular volume/unit-cell volume.

Interaction (*X*—H···*Y*)	Interatomic distances (Å)				
	X···*Y*	H···*Y*	*X*—H···*Y* (°)	Symmetry of *Y*	Structural level
(2): $C_k = 0.68$					
N(2)—H(2)···N(2)	2.899 (14)	2.12 (12)	168 (6)	$2-x, 1-x+y, \frac{1}{2}-z$	(2)
N(2)—H(2)···Π(1-5)	4.041 (11)	3.17 (9)	170 (9)	$2-x+y, 1-x, z$	(3)
C(6)—H(61)···H(4)	3.20 (8)	2.65 (12)	118 (9)	$1-x, x-y, z$	(3)
C(6)—H(61)···H(61)	2.96 (8)	2.04 (12)	172 (10)	$2-x, 1-x+y, \frac{1}{2}-z$	(3)
C(6)—H(63)···H(63)	3.41 (9)	2.56 (11)	119 (7)	$\frac{1}{3}+y, \frac{2}{3}-x+y, \frac{2}{3}-z$	(3)
C(6)—H(63)···H(63)	3.36 (10)	2.56 (12)	139 (6)	$\frac{1}{3}+x-y, -\frac{1}{3}+x, \frac{2}{3}-z$	(3)
C(6)—H(61)···Π(1-5)	3.721 (9)	3.58 (8)	92 (5)	$\frac{5}{3}-x, \frac{1}{3}-y, \frac{1}{3}-z$	(4)
C(6)—H(61)···Π(1-5)	4.459 (9)	3.92 (8)	120 (6)	$\frac{1}{3}+x-y, -\frac{1}{3}+x, \frac{2}{3}-z$	(4)
C(6)—H(62)···Π(1-5)	3.721 (9)	3.13 (8)	121 (7)	$\frac{5}{3}-x, \frac{1}{3}-y, \frac{1}{3}-z$	(4)
(5): $C_k = 0.66$					
N(1*A*)—H(1*A*)···N(2*B*)	2.858 (4)	1.87 (9)	168 (6)	x, y, z	(2)
N(1*B*)—H(1*B*)···N(2*C*)	2.872 (4)	2.02 (9)	159 (8)	x, y, z	(2)
N(1*C*)—H(1*C*)···N(2*A*)	2.880 (3)	1.97 (9)	167 (6)	x, y, z	(2)
N(2*A*)—H(2*A*)···N(1*C*)	2.880 (3)	1.96 (8)	177 (9)	x, y, z	(2)
N(2*B*)—H(2*B*)···N(1*A*)	2.858 (4)	2.15 (8)	172 (9)	x, y, z	(2)
N(2*C*)—H(2*C*)···N(1*B*)	2.872 (4)	2.16 (8)	167 (7)	x, y, z	(2)
C(3*A*)—H(3*A*)···O(8*B*)	3.341 (4)	2.51 (4)	168 (3)	$x, 1+y, -1+z$	(3)
C(5*A*)—H(5*A*)···O(7*C*)	3.302 (4)	2.44 (4)	167 (5)	$-1+x, -1+y, z$	(3)
C(3*B*)—H(3*B*)···O(8*C*)	3.347 (4)	2.45 (4)	174 (4)	$-1+x, -1+y, z$	(3)
C(5*B*)—H(5*B*)···O(7*A*)	3.285 (4)	2.43 (4)	176 (4)	$1+x, y, 1+z$	(3)
C(3*C*)—H(3*C*)···O(8*A*)	3.336 (5)	2.40 (4)	169 (3)	$1+x, y, 1+z$	(3)
C(5*C*)—H(5*C*)···O(7*B*)	3.286 (4)	2.34 (4)	172 (3)	$x, 1+y, -1+z$	(3)
N(1*A*)—H(1*A*)···Π(1-5)*A*	3.617 (4)	3.78 (10)	73 (5)	$-x, 1-y, -z$	(4)
N(2*A*)—H(2*A*)···Π(1-5)*A*	3.355 (4)	3.27 (10)	87 (7)	$-x, 1-y, -z$	(4)
N(1*C*)—H(1*C*)···Π(1-5)*A*	3.961 (3)	3.57 (12)	108 (7)	$-x, 1-y, -z$	(4)
C(5*A*)—H(5*A*)···Π(1-5)*B*	4.482 (4)	3.85 (5)	131 (4)	$-x, -y, -z$	(4)
N(1*B*)—H(1*B*)···Π(1-5)*C*	3.971 (3)	3.60 (10)	108 (8)	$1-x, 1-y, -z$	(4)
N(1*C*)—H(1*C*)···Π(1-5)*C*	3.620 (4)	3.72 (12)	77 (7)	$1-x, 1-y, -z$	(4)
N(2*C*)—H(2*C*)···Π(1-5)*C*	3.361 (4)	3.29 (9)	89 (7)	$1-x, 1-y, -z$	(4)
Π(1-5)*A*···Π(1-5)*A*	3.688 (2)	—	0	$-x, 1-y, -z$	(4)
Π(1-5)*C*···Π(1-5)*C*	3.737 (2)	—	0	$1-x, 1-y, -z$	(4)
(6): $C_k = 0.65$					
N(1)—H(1)···N(2)	2.889 (14)	2.12 (12)	168 (6)	$y, x, 1-z$	(2)
C(7)—H(7*B*)···O(9)	3.455 (20)	2.55 (24)	140 (12)	$1-x, 1-x+y, \frac{1}{3}-z$	(3)
C(7)—H(7*A*)···H(7*A*)	3.29 (15)	2.59 (12)	140 (10)	$y, x, 1-z$	(3)
(1): $C_k = 0.66$					
N(1*A*)—H(1*A*)···N(2*B*)	2.914 (6)	1.90 (8)	164 (7)	x, y, z	(2)
N(1*B*)—H(1*B*)···N(2*A*)	2.902 (6)	1.89 (8)	179 (7)	$x, \frac{3}{2}-y, -\frac{1}{2}+z$	(2)
C(3*A*)—H(3*A*)···Π(1-5)*A*	3.688 (6)	2.64 (2)	165 (1)	$x, \frac{3}{2}-x, \frac{1}{2}+z$	(2)
C(5*B*)—H(5*B*)···Π(1-5)*B*	3.554 (6)	2.55 (2)	151 (1)	$x, \frac{3}{2}-x, -\frac{1}{2}+z$	(2)
C(3*B*)—H(3*B*)···Π(1-5)*A*	3.926 (6)	2.99 (2)	145 (1)	$\frac{1}{2}+x, 1-y, 1-z$	(3)
C(5*A*)—H(5*A*)···Π(1-5)*B*	3.681 (6)	2.67 (1)	151 (1)	$-\frac{1}{2}+x, 1-y, -z$	(3)

The packing in the structure of (5) is a slight deformation of that of (2) and yet dramatically changes the descriptive symmetry. This packing of (5) is pseudo-rhombohedral, with new axes $A = c - b$, $B = a + b$ and $C = b + c - a$ (see Table 11 and Fig. 3), very similar to those of (2), which lacks the NO_2 group but bears methyl groups at positions 3 and 5. The packing also presents sheets of trimers; there are six sheets per *C* axis, giving 3.193 Å intersheets and 119.87 Å^2 per trimer (the pseudo-hexagonal base area). Again the trimers (see Table 9), including the disordered H atoms, are held by hydrogen bonds, while here the sheets are formed by C—H···O_2N interactions (3*ry S*) and the sheets are compacted to give the crystal by ring/H···ring interactions. All trimers are equally oriented within a sheet; the center of trimers and the orientation of them with respect to the *A* axis (+ or −, one with respect to each other sheet as in the star of David) in the six sheets are: (2/3,0;−), (0,1/3;+), (1/3,1/3;−), (2/3,2/3;+), (0,2/3;−) and (1/3,0,+), while for (2) the positions and orientations are: (2/3,1/3;+), (0,0;−) (1/3,2/3;+), (2/3,1/3;−), (0,0;+) and (1/3,2/3;−), both having in the middle a center of symmetry.

Opening the trimers of (2) and rearranging the hydrogen bonds (2*ry S*) we obtain the packing of (6), which is very similar, in the projection along *c*, to a sheet of (2) (see Fig. 4) and with similar *a*- and *b*-axes

Table 10. *Main interactions building the packing in the structures of* (3), (4), (7) *and* (8), *showing the symmetry involved in the interaction and, in parentheses, the corresponding structural level*

Π represents the centroid of the indicated ring. C_k is the total packing coefficient as measured by the ratio: van der Waals' molecular volume/unit-cell volume.

	Interatomic distances (Å)				
Interaction (X—H···Y)	X···Y	H···Y	X—H···Y (°)	Symmetry of Y	Structural level
(7): $C_k = 0.67$					
N(1)—H(1)···N(2)	3.012 (2)	2.32 (3)	141 (2)	$1-x, 1-y, 1-z$	(2)
N(1)—H(1)···O(12)	3.132 (3)	2.69 (3)	115 (2)	$x, \frac{1}{2}-y, \frac{1}{2}+z$	(3)
C(9)—H(9*B*)···O(12)	3.580 (2)	2.62 (3)	155 (2)	$x, \frac{1}{2}-y, \frac{1}{2}+z$	(3)
C(9)—H(9*A*)···O(11)	3.575 (2)	2.68 (3)	148 (3)	$-x, \frac{1}{2}+y, \frac{1}{2}-z$	(3)
C(8)—H(8*B*)···O(11)	3.584 (3)	2.73 (4)	149 (3)	$-x, \frac{1}{2}+y, \frac{1}{2}-z$	(3)
C(14)—H(14*A*)···O(11)	3.676 (3)	2.73 (4)	158 (3)	$1-x, \frac{1}{2}+y, \frac{1}{2}-z$	(3)
C(8)—H(8*A*)···H(9*A*)	3.63 (3)	2.75 (5)	151 (3)	$-x, -\frac{1}{2}+y, \frac{1}{2}-z$	(3) or (4)
C(8)—H(8*C*)···H(14*C*)	3.60 (4)	2.74 (6)	140 (3)	$1-x, \frac{1}{2}+y, \frac{1}{2}-z$	(3) or (4)
C(8)—H(8*C*)···H(16*C*)	3.51 (4)	2.69 (6)	136 (3)	$1-x, \frac{1}{2}+y, \frac{1}{2}-z$	(3) or (4)
C(7)—H(7*A*)···H(15*C*)	3.43 (4)	2.70 (6)	132 (3)	$-1+x, y, z$	(3) or (4)
C(9)—H(9*B*)···H(15*B*)	2.84 (4)	2.43 (5)	103 (2)	$1-x, 1-y, 1-z$	(3) or (4)
C(9)—H(9*C*)···H(15*B*)	2.84 (4)	2.46 (5)	101 (2)	$1-x, 1-y, 1-z$	(3) or (4)
C(9)—H(9*C*)···H(14*C*)	3.37 (5)	2.43 (6)	153 (3)	$1-x, \frac{1}{2}+y, \frac{1}{2}-z$	(3) or (4)
C(14) − H(14*A*)···H(16*A*)	3.22 (4)	2.62 (5)	118 (3)	$1-x, \frac{1}{2}+y, \frac{1}{2}-z$	(3) or (4)
C(16)—H(16*B*)···H(16*B*)	3.40 (6)	2.60 (8)	147 (4)	$1-x, -y, 1-z$	(3) or (4)
(3): $C_k = 0.57$					
N(1)—H(1)···N(2)	2.900 (5)	1.99 (–)	149 (–)	$1-x, -y, 1-z$	(2)
C(11)—H(11*A*)···C(8)	3.916 (19)	3.16 (–)	131 (–)	$\frac{1}{2}+x, \frac{1}{2}-y, 1-z$	(3) or (4)
C(11)—H(11*B*)···C(9′)	3.800 (25)	3.40 (–)	105 (–)	$x, \frac{1}{2}-y, \frac{1}{2}+z$	(3) or (4)
C(12)—H(12*A*)···C(8)	3.956 (21)	3.16 (–)	154 (–)	$\frac{1}{2}+x, \frac{1}{2}-y, 1-z$	(3) or (4)
C(12)—H(12*B*)···C(9′)	3.728 (24)	3.13 (–)	121 (–)	$\frac{1}{2}+x, y, \frac{1}{2}-z$	(3) or (4)
C(12)—H(12*C*)···C(9′)	3.728 (24)	3.17 (–)	114 (–)	$\frac{1}{2}+x, y, \frac{1}{2}-z$	(3) or (4)
C(12)—H(12*C*)···C(8)	4.176 (22)	3.35 (–)	136 (–)	$\frac{1}{2}+x, y, \frac{1}{2}-z$	(3) to (4)
C(13)—H(13*B*)···C(9)	3.857 (29)	3.08 (–)	137 (–)	$\frac{1}{2}-x, -y, \frac{1}{2}+z$	(3) or (4)
C(13)—H(13*C*)···C(10′)	4.066 (25)	3.03 (–)	168 (–)	$1-x, -y, 1-z$	(3) or (4)
(8): $C_k = 0.71$					
N(101)—H(101)···N(102)	3.017 (6)	2.32 (7)	124 (5)	$-x, 1-y, -z$	(2)
N(201)—H(201)···N(302)	3.023 (12)	2.33 (–)	132 (–)	$x, -\frac{1}{2}-y, \frac{1}{2}+z$	(2)
N(301)—H(301)···N(202)	3.020 (12)	2.31 (–)	134 (–)	$x, -\frac{1}{2}-y, -\frac{1}{2}+z$	(2)
N(101)—H(101)···O(119)	3.340 (6)	2.68 (7)	123 (5)	$x, \frac{1}{2}-y, \frac{1}{2}+y$	(3)
N(201)—H(201)···O(319)	3.374 (13)	2.85 (–)	118 (–)	$1-x, -y, 1-z$	(3)
N(301)—H(301)···O(219)	3.388 (13)	2.97 (–)	110 (–)	$1-x, -y, -z$	(3)
C(111)—H(111)···O(120)	3.583 (7)	2.55 (7)	167 (6)	$-x, -y, -z$	(4)
C(108)—H(108)···O(120)	3.533 (7)	2.79 (11)	136 (8)	$-x, \frac{1}{2}+y, -\frac{1}{2}-z$	(4)
C(211)—H(211)···O(320)	3.633 (8)	2.65 (6)	158 (4)	$x, \frac{1}{2}-y, \frac{1}{2}+z$	(4)
C(208)—H(208)···O(220)	3.494 (3)	2.76 (13)	140 (10)	$1-x, -\frac{1}{2}+y, \frac{1}{2}-z$	(4)
C(310)—H(310)···O(320)	3.472 (12)	2.76 (9)	138 (6)	$1-x, -\frac{1}{2}+y, \frac{1}{2}-z$	(4)
C(308)—H(308)···Π(106–111)	3.664 (7)	2.88 (8)	136 (6)	$1+x, \frac{1}{2}-y, \frac{1}{2}+z$	(4)
C(116)—H(116)···Π(306–311)	3.759 (7)	2.84 (9)	146 (6)	$1-x, \frac{1}{2}+y, \frac{1}{2}-z$	(4)
C(110)—H(110)···Π(206–211)	3.737 (7)	2.94 (8)	140 (7)	$-x, -y, -z$	(4)
(4): $C_k = 0.66$					
N(1*A*)—H(1*A*)···N(1*A*)	2.892 (3)	1.90 (–)	154 (–)	$1-x, y, \frac{1}{2}-z$	(2)
N(2*A*)—H(2*A*)···N(2*B*)	2.835 (3)	1.90 (–)	154 (–)	$1-x, y, \frac{1}{2}-z$	(2)
N(1*B*)—H(1*B*)···N(1*B*)	2.915 (3)	1.92 (–)	165 (–)	$1-x, y, \frac{1}{2}-z$	(2)
N(2*B*)—H(2*B*)···N(2*A*)	2.835 (3)	1.87 (–)	156 (–)	$1-x, y, \frac{1}{2}-z$	(2)
C(16*B*)—H(16*B*)···Π(6–11)*A*	3.742 (6)	3.18 (5)	118 (3)	x, y, z	(3)
C(9*B*)—H(9*B*)···Π(6–11)*A*	4.593 (6)	3.69 (5)	152 (3)	$\frac{1}{2}+x, \frac{1}{2}-y, -\frac{1}{2}+z$	(3)
C(9*A*)—H(9*A*)···Π(12–17)*A*	3.784 (6)	3.02 (4)	139 (3)	$\frac{1}{2}-x, -\frac{1}{2}+y, \frac{1}{2}-z$	(3)
C(11*A*)—H(11*A*)···Π(12–17)*A*	4.453 (4)	3.55 (4)	152 (3)	$\frac{1}{2}-x, \frac{1}{2}-y, -z$	(3)
C(13*B*)—H(13*B*)···Π(6–11)*B*	3.529 (5)	3.00 (4)	175 (2)	$1-x, -y, -z$	(3)
C(9*B*)—H(9*B*)···Π(6–11)*A*	4.593 (6)	3.69 (5)	152 (3)	$\frac{1}{2}+x, \frac{1}{2}-y, -\frac{1}{2}+z$	(3)
C(4*A*)—H(4*A*)···Π(6–11)*B*	4.436 (3)	3.54 (4)	157 (3)	$\frac{1}{2}-x, \frac{1}{2}-y, -z$	(3)
C(11*A*)—H(11*A*)···Π(6–11)*B*	4.157 (4)	3.53 (4)	123 (3)	$\frac{1}{2}-x, \frac{1}{2}-y, -z$	(3)
C(14*A*)—H(14*A*)···Π(12–17)*B*	4.010 (5)	3.28 (4)	135 (3)	$\frac{1}{2}-x, \frac{1}{2}-y, -z$	(3)
C(10*B*)—H(10*B*)···Π(12–17)*B*	4.054 (4)	3.18 (4)	144 (3)	$x, -y, -\frac{1}{2}+z$	(3)
C(8*A*)—H(8*A*)···Π(12–17)*B*	4.830 (5)	3.97 (6)	139 (4)	$x, -y, \frac{1}{2}+z$	(3)
C(8*A*)—H(8*A*)···Π(12–17)*A*	4.022 (6)	3.49 (6)	112 (3)	$\frac{1}{2}-x, -\frac{1}{2}+y, \frac{1}{2}-z$	(3)

(see Table 11). Packing of (6) presents a secondary structure of a helix along the *c*-axis through hydrogen bonds, with a tertiary structure linking the helices by H···H and H···O_2N interactions (see Table 9) and producing a crystal with no quaternary structure. The packing presents three molecules per *c*-axis, each corresponding to one sheet of (2); which gives 1.361 Å interlevels and 129.43 $Å^2$ per helix (the base

Table 11. *Unit-cell parameters of the eight compounds presented in this work*

For (5), the table shows the parameters for the pseudo-rhombohedral cell (*).

	Lattice			Angles			Symmetry
(1)	8.232	12.840	7.054	90.0	90.0	90.0	$P2_1cn$
(6)	12.225	12.225	4.083	90.0	90.0	120.0	$P3_121$
(5)	9.883	9.669	8.342	81.1	100.1	106.0	$P\bar{1}$
(5)*	11.757	11.773	19.158	91.6	99.1	120.0	R
(2)	11.775	11.775	20.991	90.0	90.0	120.0	$R\bar{3}c$
(3)	11.478	21.100	9.980	90.0	90.0	90.0	$Pbca$
(7)	10.641	9.618	12.665	90.0	108.0	90.0	$P2_1/c$
(8)	18.140	12.081	11.518	90.0	99.4	90.0	$P2_1/c$
(4)	16.923	17.143	17.640	90.0	109.6	90.0	$C2/c$

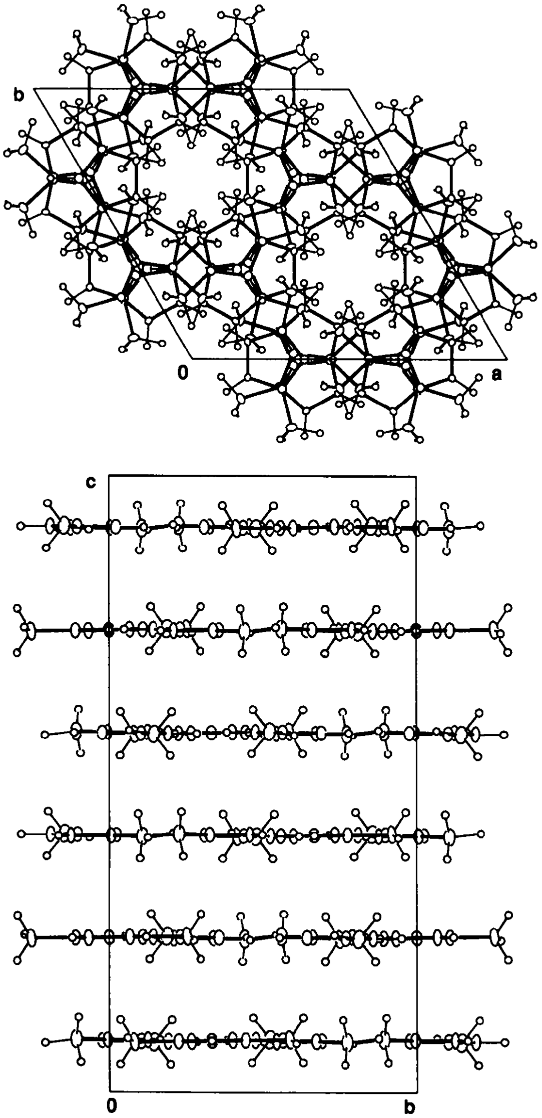

Fig. 2. Two views of the packing of (2), showing the six sheets per *c* axis. One isolated sheet is very similar to the projection of the structure of (6) shown in Fig. 4.

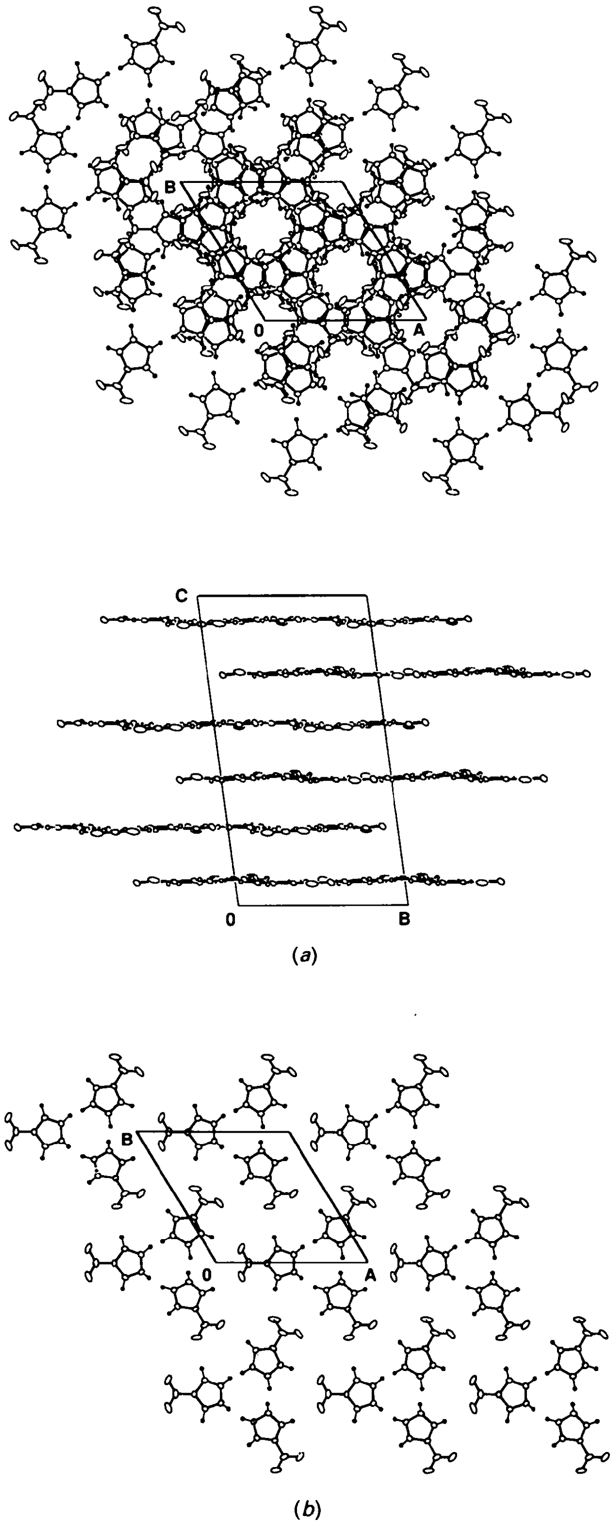

(*a*)

(*b*)

Fig. 3. (*a*) Same as Fig. 2, but for (5), in the pseudo-rhombohedral unit cell ($A = c - b$, $B = a + b$ and $C = b + c - a$), showing the shift in the sheets with respect to that of (2). (*b*) A sheet of (5), that referred to as (2/3,0;−), showing the positions of the trimer.

area). So, it seems that the helix would collapse into one of the sheets of (2), since leaving out the methyl groups provides more space.

Again, in (1), the secondary structure is formed by two hydrogen bonds (see Table 9 and Fig. 5), which give rise to a helix along the *c*-axis that hold four units per *c*-axis. The helices are joined to give the crystal (3*ry S* with no 4*ry S*) through two C—H···ring interactions (see Table 9); the other two ring interactions reinforce the helix system, twisting it so as to give the eight shaped chains. The structure can be considered as having a noncrystallographic rhombic base, with $2A = a + b$, $2B = a - b$ and $C = c$, $A = B = 7.626$ Å and $\gamma' = 114.67°$, so as to give 1.7864 Å per unit as the pitch value and 52.58 Å^2 per helix.

A different mode of packing is present in the structures of (3), (4), (7) and (8); it consists of dimers [or a tetramer in (4)] for the secondary structure; these form tertiary sheets; the crystal is then built (4*ry S*) by compacting the sheets.

Compound (7) presents a secondary structure formed by dimers through hydrogen bonds (see Table 10 and Fig. 6). The presence of NO_2 groups allows these hydrogen bonds to bifurcate in planes parallel to *b*,*c* to form sheets (3*ry S*), reinforced by some H···H contacts. The sheets build the crystal (4*ry S*) through a methyl-crowded zone perpendicular to the *a*-axis.

Compound (3) presents a packing quite similar to that of (7) (see Table 10 and Fig. 7), with a secondary structure made of dimers through hydrogen bonds, sheets parallel to the *a*,*b*-plane, as in the tertiary structure, and a methyl-full zone perpendicular to *c*.

Compound (8) has a packing made of slabs across *a*, alternately ordered and disordered (see Fig. 8). Here, again, we have a secondary structure made of dimers produced by hydrogen bonds. The dimers link among themselves by H···O_2N interactions, producing sheets parallel to the *b*,*c*-plane. The rest of the interactions, see Table 10 (including the phenyl–phenyl interactions, which are of the 'T'-type with an average angle of 55°), link the different sheets along the ⟨101⟩ direction, asymmetrizing the molecular interactions around the ordered molecule, while the disordered interactions present a symmetric neighborhood.

The structure of (4) is made of sheets approximately normal to ⟨101⟩ (see Fig. 9). The secondary structure is made of tetramers, in an 'eight'-like

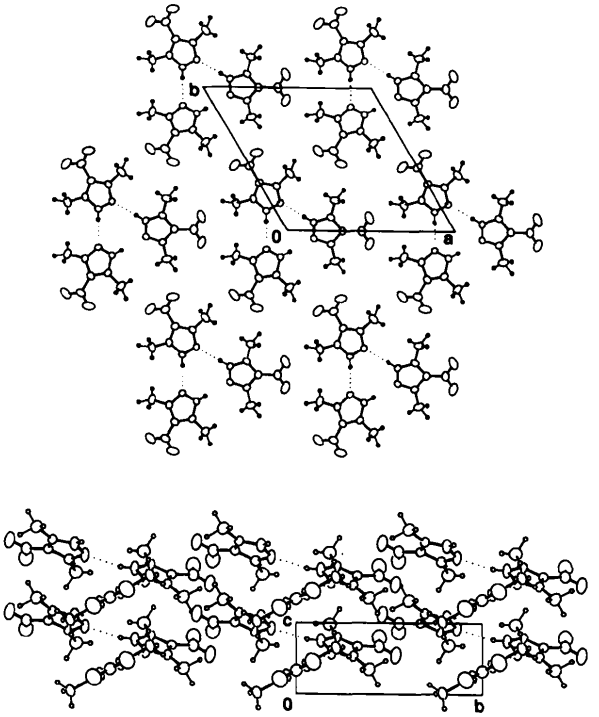

Fig. 4. The packing of (6), showing the helices of the secondary structure, while the projection along *c* is like a sheet in (2) or (5).

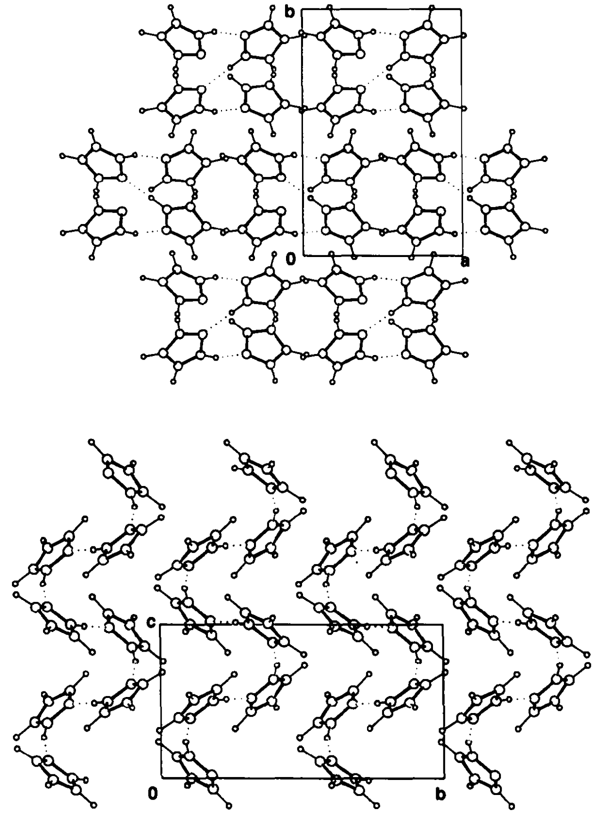

Fig. 5. The packing of (1). The helices are distorted from those of (6) so as to give a quite different projection along *c*.

fashion, that links two adjacent sheets. Within each sheet, the H···phenyl interactions (see Table 10) are linking the molecules, which are in a quasi-perpendicular situation. The sheets present individually the same structure, but one is sheared with respect to the other.

Relationships between crystallography and thermodynamic properties

The structural information gathered from the X-ray analysis is relevant both to the molecular properties of the isolated molecules and to those of the solid.

Table 12. *Acid–base equilibria of pyrazoles*

Acid–base properties	Basic pK_a	Acid pK_a
Pyrazole (1)	2.48	14.21
3,5-Dimethylpyrazole (2)	4.06	15.00
3,5-Di-*tert*-butylpyrazole (3)	3.94	15.13
3,5-Diphenylpyrazole (4)	1.75	13.03
4-Nitropyrazole (5)	−2.0	0.64
3,5-Dimethyl-4-nitropyrazole (6)	−0.45	10.65
3,5-Di-*tert*-butyl-4-nitropyrazole (7)	−0.12	11.29
3,5-Diphenyl-4-nitropyrazole (8)	—	—

Among the first are the acid–base properties of pyrazoles (Catalán, Abboud & Elguero, 1987). We report in Table 12 the pK_a corresponding to equilibria pzH + $H^+ \rightleftarrows pzH_2^+$ (basic pK_a) and pzH $\rightleftarrows$ pz^- + H^+ (acid pK_a), where pzH is any NH-pyrazole. The values in italics in Table 12 have been calculated from (1), which relates both pK_a's

$$\text{acid p}K_a = 11.4 + 0.946\ \text{basic p}K_a,\ r^2 = 0.98. \qquad (1)$$

Unfortunately, the data for (8) are missing and cannot be estimated.

From the pairs (1)–(5) and (2)–(6) the effect of a 4-nitro substituent on the acid–base equilibria can be calculated: Basicity δpK_a = −4.50, acidity δpK_a = −4.46. In the case of the (3)–(7) pair, these values are −4.06 and −3.84, respectively. We assign these differences ($\delta\delta$pK_a = +0.44 and +0.62) to the twist of the nitro group in (7) [θ = C(3)—C(4)—N(3)—O(1) = 45.7°], which modifies its electronic properties. When θ changes from near 0°, (5) and (6), to

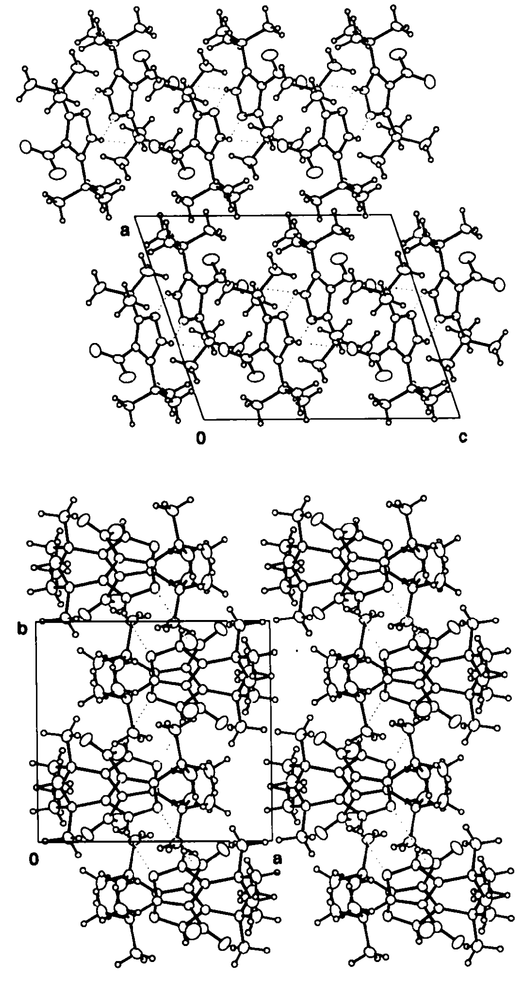

Fig. 6. The packing of (7), showing the secondary structure due to hydrogen-bonded dimers and the methyl-crowded zone.

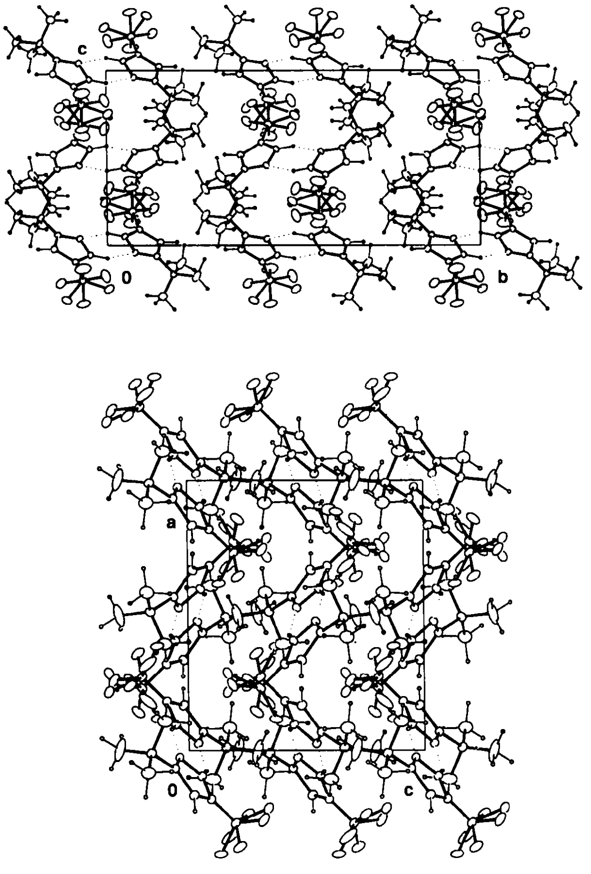

Fig. 7. Same as in Fig. 6 but for (3).

46°, (7), the nitro group loses part of its electron-withdrawing ability and the pyrazole becomes relatively more basic and less acidic in character. Concerning the (4)–(8) pair, since the nitro group is almost planar ($\theta \sim 0°$), one may expect δpK_a values near -4.5 units. The twist of the phenyl rings, greater in (8) and (4) (Table 7), could affect the pK_a values.

Concerning the thermodynamical properties of the crystal as a whole, we have tried to link up the heats of sublimation and the crystal structure. This is an old and difficult problem. The enthalpy of sublimation at a given temperature is related to the lattice energy U by (2) (Giacovazzo *et al.*, 1992)

$$\Delta_{\rm sub}H^0\,m(T) = U + K_0 + 2RT, \qquad (2)$$

where K_0, the zero-point energy, is usually very small and $2RT \simeq 5$ kJ mol^{-1} at 298.15 K. Thus, in a first approximation, the data of Table 2 can be transformed into lattice energies by simply adding 5 kJ mol^{-1} to each value. This is not necessary, since we will discuss only relative values, $\delta\Delta_{\rm sub}H^0m(T) = \delta U$.

The lattice energy can be decomposed into three terms (Giacovazzo *et al.*, 1992)

$$U = \text{nonbonded energy} + \text{electrostatic energy} + \text{hydrogen bonding} \qquad (3)$$

Instead of calculating these terms, we will try an empirical approach, our goal being to estimate the hydrogen-bonding term ($E_{\rm HB}$ hereinafter), since the most characteristic property of the NH-pyrazoles is

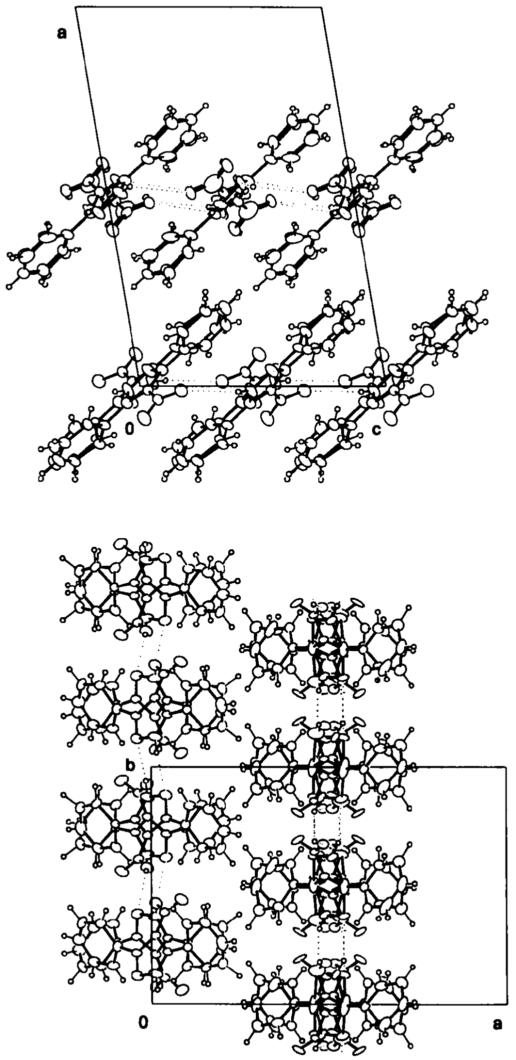

Fig. 8. The packing of (8), showing the alternate ordered and disordered sheets. The methyl-crowded zones have been substituted by phenyl-crowded ones.

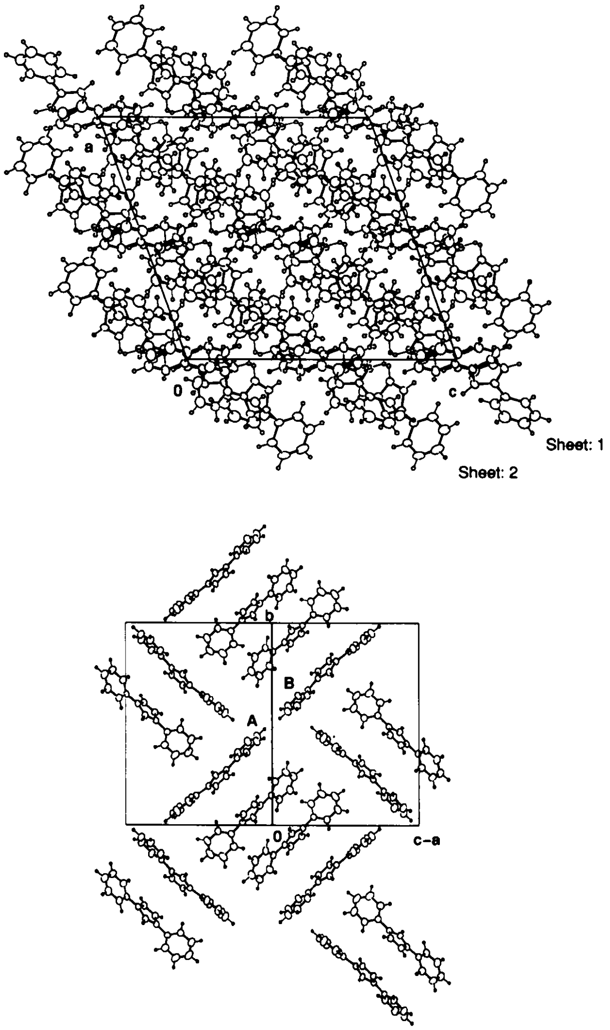

Fig. 9. The slabs in the packing of (4). One sheet (sheet 1) is shown beneath, the other being this one shifted so as to superimpose molecule *A* with molecule *B*.

the hydrogen-bond network they form when crystallizing.

One first possible approach is to search for relationships between the sublimation enthalpies and some global crystallographic property, such as density, packing function, cell volume *etc.* This approach, for homologous series, is not as far-fetched as it may appear. For heats of vaporization, it has been shown (Cox & Pilcher, 1970) that (4) holds for families of compounds

$$[L] = M_w \times \Delta H^{0.8}/(D_l - D_V), \qquad (4)$$

where L is a constant, characteristic of the family, M_w is the molecular weight, and $D_l - D_V$ are the densities of the liquid and vapor. A similar equation for the heat of sublimation of crystals would have the form of (5), assuming that $D_c >\!>\!> D_V$

$$\Delta_{\rm sub}H^0 = ([L] \times D_c)/M_w. \qquad (5)$$

We have represented in Fig. 10 the scatterplot of $\Delta_{\rm sub}H^2$ *versus* D_c/M_w. Some trends are apparent: pyrazoles substituted by H, CH_3 and $^tC_4H_9$ groups [(1), (2) and (3)] are situated in a straight line with the slope $[L] = -1828$, *i.e.* when the ratio density/molecular weight increases, the heat of sublimation decreases. The introduction of a nitro group at position 4 [(5), (6) and (7)] displaces the line towards higher values of $\Delta_{\rm sub}H^0$, but clearly all these compounds belong to the same family. This is not the case for 3,5-diphenyl derivatives (4) and (8), which behave differently. In all cases, the introduction of a nitro group increases the sublimation enthalpy without modifying the D_c/M_w ratio (3–7, 4–8) or even decreasing it (1–5, 2–6). More examples are needed to confirm these observations or to find another trend.

The relationships represented in Fig. 1 and (3) are mutually consistent only if the $E_{\rm HB}$ term, absent in benzenes, is constant for all the eight pyrazoles. The two compounds which show the largest deviation from the regression line are (5) ($\delta\Delta_{\rm sub}H^0$), higher than expected, and (4) ($\delta\Delta_{\rm sub}H^0$), lower than expected. If these differences arise from the $E_{\rm HB}$ term, then in (4) (3,5-di-*tert*-butylpyrazole), the HB network is weaker than in other pyrazoles and the opposite for (5) (4-nitropyrazole).

The possibility that the $E_{\rm HB}$ term is not constant, but too small to be significant, can be ruled out on the following considerations. No direct determination of the strength of the hydrogen bonds in NH-pyrazoles is known, but it is possible to estimate its energy by molecule. The N—H···N bond in ammonia (it is important to use neutral molecules) amounts to 16 kJ mol^{-1} (Bradley & Cleasby, 1953), 37 kJ mol^{-1} in the imidazole catamer (*ab initio* calculations) (Brédas, Poskin, Delhalle, André & Chojnaki, 1984) and for pyrazole we have calculated 18 kJ mol^{-1} (Clementi, Corongiu, de Paz & Elguero, 1995). Since $\Delta_{\rm sub}H^2$ of pyrazole is 74 kJ mol^{-1}, it is evident that the contribution of $E_{\rm HB}$ to U is important and cannot be neglected. Recently (da Silva & Monte, 1992), it has been described that for a series of six halogen-substituted 8-hydroxyquinolines, there is linear relationship between [$\Delta_{\rm sub}H^0_m$ ($T_{0.5\,\rm Pa}$)/kJ mol^{-1}] and T (0.5 Pa), where T (0.5 Pa) is the temperature at which the equilibrium pressure of each substance is 0.5 Pa. To check if this empirical

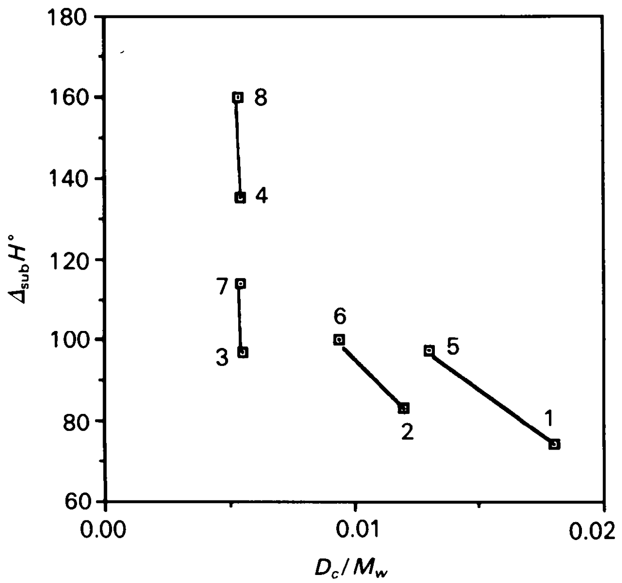

Fig. 10. Plot of $\Delta_{\rm sub}H^\circ$ *versus* D_c/M_w for pyrazoles (1)–(8).

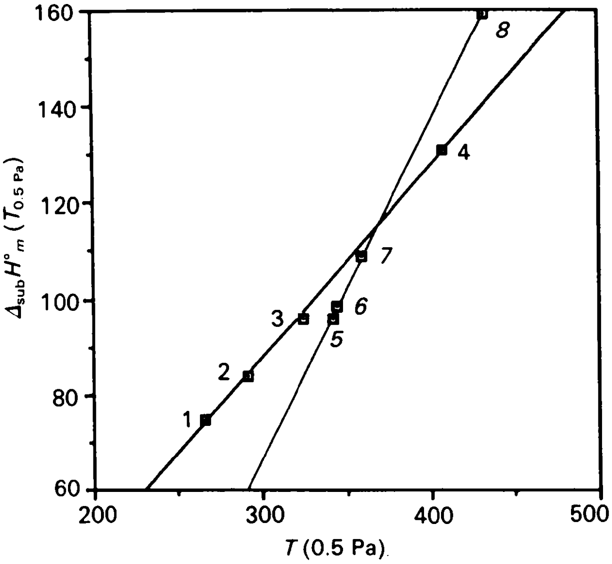

Fig. 11. Dependence of the standard molar enthalpy of sublimation $\Delta_{\rm sub}H^\circ_m$ ($T_{0.5\,\rm Pa}$) on the temperature of sublimation T (0.5 Pa).

relationship is followed by pyrazoles we have calculated these values (Table 2). The corresponding plot (Fig. 11) shows two perfect straight lines, one for H-4 pyrazoles [$\Delta_{\rm sub}H^0{}_m(T_{0.5\ \rm Pa})/{\rm kJ\ mol}^{-1} = -31.57 + 0.3968\ T(0.5\ {\rm Pa})$, $n = 4$, $R = 1.00$] and the other for 4-nitropyrazoles [$\Delta_{\rm sub}H^0{}_m(T_{0.5\ \rm Pa})/{\rm kJ\ mol}^{-1} = -141.75 + 0.6966 + 0.3968\ T(0.5\ {\rm Pa})$, $n = 4$, $R = 1.00$]. In the case of da Silva & Monte (1992), the slope is 0.313.

Concluding remarks

NH-Pyrazoles are some of the simplest bifunctional heteroaromatic compounds (others include NH-imidazoles): they have a hydrogen-bond donor group (HBD), the N—H, and a hydrogen-bond acceptor group (HBA), the N(2) atom, which are of paramount importance for determining their solid-state secondary structure. Nevertheless, the case of compounds (1–8) proves to be too complex for quantitative analysis. Not only as many packing patterns as different pyrazoles were observed, but no rules have been found to predict the order–disorder dichotomy of the N—H···N intermolecular hydrogen bond, which determined the dynamic properties of these crystals (Part II, Limbach *et al.*, 1995). Moreover, the challenge of establishing relationships between the heats of sublimation and the crystal structure has been only partly met.

Thanks are given to the DGICYT of Spain (Project Number PB93-0125) and to the EEC [Science Program, Project Number SCI.0045C(H)] for financial support. We also thank one of the referees to point out to us the reference by da Silva & Monte (1992), which led to Fig. 11.

References

Abrahams, S. C. & Keve, E. T. (1971). *Acta Cryst.* **A27**, 157–165.

Aguilar-Parrilla, F., Cativiela, C., Villegas, M. D. D. de, Elguero, J., Foces-Foces, C., Laureiro, J. I. G., Cano, F. H., Limbach, H. H., Smith, J. A. S. & Toiron, C. (1992). *J. Chem. Soc. Perkin Trans* 2, pp. 1737–1742.

Aguilar-Parrilla, F., Limbach, H. H., Foces-Foces, C., Cano, F. H. & Elguero, J. (1994). *J. Org. Chem.* Submitted.

Aguilar-Parrilla, F., Scherer, G., Limbach, J. H., Foces-Foces, C., Cano, F. H. & Elguero, J. (1992). *J. Am. Chem. Soc.* **114**, 9657–9659.

Babar, V. J., Desai, B. J. & Shinde, V. M. (1983). *J. Indian Chem. Soc.* **60**, 896–897.

Beurskens, P. T., Bosman, W. P., Doesburg, H. M., Gould, R. O., van den Hark, Th. E. M., Prick, P. A. J., Noordik, J. H., Beurskens, G., Parthasarthi, V., Bruins Slot, H. J., Haltiwanger, R. C. & Smits, J. M. M. (1984). *DIRDIF System.* Crystallography Laboratory, Toernooiveld, 6525 ED Nijmegen, The Netherlands.

Bradley, R. S. & Cleasby, T. G. (1953). *J. Chem. Soc.* pp. 1681–1684.

Brédas, J. L., Poskin, M. P., Delhalle, J., André, J. M. & Chojnaki, H. (1984). *J. Phys. Chem.* **88**, 5882–5887.

Burla, M. C., Camalli, M., Cascarano, G., Giacovazzo, C., Polidori, G., Spagna, R. & Viterbo, D. (1989). *J. Appl. Cryst.* **22**, 389–393.

Catalán, J., Abboud, J. L. M. & Elguero, J. (1987). *Adv. Hetercycl. Chem.* **41**, 187–274.

Clementi, E., Corongiu, G., de Paz, J. L. G. & Elguero, J. (1995). In preparation.

Colomina, M., Jiménez, P. & Turrión, C. (1982). *J. Chem. Thermodyn.* **14**, 779–784.

Cox, J. D. & Pilcher, G. (1970). *Thermochemistry of Organic and Organometallic Compounds*, p. 120. London: Academic Press.

Domenicano, A. & Murray-Rust, P. (1979). *Tetrahedron Lett.* pp. 2283–2286.

Elguero, J. (1984). Pyrazoles and their benzo derivatives, in *Comprehensive Heterocyclic Chemistry*, edited by A. R. Katritzky & C. W. Rees, Vol. 5, pp. 167–303. Oxford: Pergamon Press.

Elguero, J., Jacquier, R. & Tien Duc, H. C. N. (1966). *Bull. Soc. Chim. Fr.* pp. 3727–3743.

Elguero, J., Yranzo, G. I., Laynez, J., Jiménez, P., Menédez, M., Catalán, J., de Paz, J. L. G., Anvia, F. & Taft, R. W. (1991). *J. Org. Chem.* **56**, 3942–3947.

Foces-Foces, C., Cano, F. H. & Elguero, J. (1993). *Gazz. Chim. Ital.* **123**, 477–479.

Foces-Foces, C., Llamas-Saiz, A. L., Claramunt, R. M., López, C. & Elguero, J. (1994). *J. Chem. Soc. Chem. Commun.* Submitted.

Frisch, M. J., Trucks, G. W., Head-Gordon, M., Gill, P. M. W., Wong, M. W., Foresman, J. B., Johnson, B. G., Schlegel, H. B., Robb, M. A., Replogle, E. S., Gomperts, R., Andres, J. L., Raghavachari, K., Binkleyu, J. S., Gonzalez, C., Martin, R. L., Fox, D. J., Defrees, D. J., Baker, J., Stewart, J. J. P. & Pople, J. A. (1992). *Gaussian*92. Revision C. Gaussian, Inc., Pittsburgh, PA, USA.

Giacovazzo, C., Monaco, H. L., Viterbo, D., Scordani, F., Gilli, G., Zanotti, G. & Catti, M. (1992). *Fundamentals of Crystallography*, edited by C. Giacovazzo. Oxford: Oxford University Press.

Habraken, C. L., Beenaker, C. I. M. & Brussee, J. (1972). *J. Heterocycl. Chem.* **9**, 939–941.

Hall, S. R., Flack, H. D. & Stewart, J. M. *Xtal*3.2 (1993). Univ. of Western Australia, Lamb, Perth.

Hehre, W. J., Radom, L., Schleyer, P. v. R. & Pople, J. A. (1986). *Ab Initio Molecular Orbital Theory.* New York: John Wiley and Sons.

Hüttel, R., Büchele, F. & Jochum, P. (1955). *Chem. Ber.* **88**, 1577–1585.

Jiménez, P., Roux, M. V. & Turrión, C. (1992). *J. Chem. Thermodyn.* **24**, 1145–1149.

Jiménez, P., Roux, M. V., Turrión, C. & Gomis, F. (1987). *J. Chem. Thermodyn.* **19**, 985–992.

LaTour, T. & Rasmussen, S. E. (1973). *Acta Chem. Scand.* **27**, 1845–1854.

Lebedeva, N. D., Katin, Yu. A. & Akhemedova, G. Ya. (1971). *Russ. J. Phys. Chem.* **45**, 1192–1194.

Limbach, H. H., Aguilar-Parrilla, F., Elguero, J., Jagerovic, N., Llamas-Saiz, A. L., Foces-Foces, C. & Cano, F. H. (1995). In preparation.

Llamas-Saiz, A. L., Foces-Foces, C. & Elguero, J. (1995). *J. Mol. Struct.* **319**, 231–260.

Llamas-Saiz, A. L., Foces-foces, C., Elguero, J. & Meutermans, W. (1992). *Acta Cryst.* **C48**, 714–717.

Martí, E. E. (1973). *Thermochim. Acta*, **5**, 173–220.

Martinez-Ripoll, M. & Cano, F. H. *PESOS*, unpublished program.

Nardelli, M. (1983). *Comput. Chem.* **7**, 95–98.

Montgomery, R. L. & Rossini, F. D. (1978). *J. Chem. Eng. Data*, **23**, 125–129.

Osborne, N. S. & Ginnings, D. C. (1947). *J. Res. Natl. Bur. Stand.* **39**, 453–477.

Prosen, E. J., Johnson, W. H. & Rossini, F. D. (1946). *J. Res. Natl. Bur. Stand.* **36**, 455–461.

Rihani, D. N. & Donaiswamy, L. K. (1965). *Ind. Eng. Chem.* pp. 17–21.

Ritchie, J. P. (1988). *Tetrahedron*, **44**, 7465–7478.

Scott, D. W., Guthrie, G. B., Messerly, J. F., Todd, S. S., Berg, W. T., Hossenlop, I. A. & McCullough, J. P. (1962). *J. Phys. Chem.* **66**, 911–914.

Silva, M. A. V. da & Monte, M. J. S. (1992). *J. Chem. Thermodyn.* **24**, 715–724.

Smith, J. A. S., Wehrle, B., Aguilar-Parrilla, F., Limbach, H. H., Foces-Foces, C., Cano, F. H., Elguero, J., Baldy, P., Pierrot, M., Khursid, M. M. T. & Lacombe-McDouall, J. R. (1989). *J. Am. Chem. Soc.* **111**, 7304–7312.

Stewart, J. M., Machin, P. A., Dickinson, C. W., Ammon, H. L., Heck, H. & Flack, H. (1976). *X-ray System of Crystallographic Programs*. Technical Report TR-446. Computer Science Center, Univ. of Maryland, College Park, Maryland, USA.

Acta Cryst. (1994). **B50**, 762–771

Structures with Identical Packing; Racemic and Partially Optically Pure 3-(2′-Chloro-2′-phenylethyl)-2-thiazolidiniminium *p*-Toluenesulfonate and a Comparison of the Packing in Corresponding Racemic and Optically Active Compounds

By Katalin Marthi and Sine Larsen

Centre for Crystallographic Studies, Department of Chemistry, University of Copenhagen, Universitetsparken 5, DK-2100 Copenhagen, Denmark

and Mária Ács,* József Bálint and Elemér Fogassy

Department of Organic Chemical Technology, Technical University of Budapest, PO Box 91, H-1521 Budapest, Hungary

(*Received 7 February 1994; accepted 28 April 1994*)

Abstract

The crystal structures have been determined for racemic and two optically active samples of 3-(2′-chloro-2′-phenylethyl)-2-thiazolidiniminium *p*-toluenesulfonate ($C_{11}H_{14}ClN_2S^+.C_7H_7O_3S^-$) from low-temperature (122 K) X-ray diffraction data. The three crystal structures are virtually identical. The racemate crystallizes in the space group $P2_1/n$, $Z = 4$, with unit-cell dimensions $a = 8.5016\,(10)$, $b = 8.2803\,(11)$, $c = 27.447\,(3)$ Å and $\beta = 96.478\,(9)°$. The cation displays disorder of the Cl atom and the C atom to which it is bonded. The disorder can be rationalized in terms of the presence of two partially populated enantiomers with different conformations. The two optically active salts contain both enantiomers of the chiral cation. The ratios between the *R*- and *S*-enantiomers were estimated to be 0.944 (7)/0.056 (7) and 0.860 (7)/0.140 (7). Both salts crystallize in the space group $P2_1$ with unit-cell dimensions almost identical to those of the racemate. The two independent anions and the ring systems of the cations are related by pseudoinversion symmetry. One of the independent cations has a disorder similar to that found for the racemate. The system of hydrogen bonds connecting two cations and two anions into 12-membered rings is identical in the racemic and in the optically active crystals. Additional evidence for the formation of a solid solution between the enantiomers and the racemate is provided by thermoanalytical and IR measurements. The crystal structures of 64 pairs of racemate and its corresponding enantiomer have been analysed. Relations similar to that observed for the salts in the present study were found for six of the pairs. For another eight pairs, there is a great resemblance between the packing of the racemate and the corresponding enantiomers.

Introduction

One of the most effective anthelmintic agents is 6-phenyl-2,3,5,6-tetrahydroimidazo[2,1-*b*]thiazole. Hydrochlorides of the racemate and the *S*-enantiomer are used as drugs and marked under the names *Tetramisole* and *Levamisole*, respectively (Negwer, 1978). The *S*-enantiomer is several times more potent but no more toxic than the *R*-isomer and is the one used to treat humans. The activity of

---

* Deceased.